Late Barremian / Early Aptian Re-Os age of the Ipubi Formation black shales: stratigraphic and paleoenvironmental implications for Araripe Basin, Northeastern Brazil

Thales Lúcio[a,*], João Adauto Souza Neto[a], David Selby[b,c]

[a] Geochemistry Laboratory Applied to Petroleum, Department of Geology, Graduate Program in Geosciences, Federal University of Pernambuco, Recife 50.740-550, Brazil <thales.lucio@ufpe.br, adauto@ufpe.br>

[b] Department of Earth Sciences, Durham University, Durham, DH13LE, UK

[c] State Key Laboratory of Geological Processes and Mineral Resources, School of Earth Resources, China University of Geosciences, Wuhan, 430074, Hubei, China

* Corresponding author. Address: Universidade Federal de Pernambuco, Centro de Tecnologia e Geociências, Departamento de Geologia, Av. da Arquitetura, s/n, Cidade Universitária, 50740-550, Recife, PE, Brasil, Tel: +55 81 997220853

Abstract

The Ipubi Formation of the Santana Group, Araripe Basin, Brazil, is characterized by black shales and overlying evaporite deposits and is suggested to record the transition from lacustrine to marine depositional environments. To date, the age of the black shales, constrained only by microfossils, is poorly determined, with ages spanning ~25 myrs from 125 to 100.5 Ma (Aptian-Albian). Here we present new Re-Os elemental and isotopic data to provide the first absolute age for those rocks of the Ipubi Formation and an improved understanding of the depositional paleoenvironment of the Araripe Basin. The Re-Os isotope data for Ipubi Formation black shales yields a depositional age of 123 ± 3.5 Ma, with a highly radiogenic initial $^{187}Os/^{188}Os$ composition (Os_i) of 1.97 ± 0.02. The Re-Os age indicates that the deposition of the Ipubi Formation black shales occurred during the Late Barremian / Early Aptian, prior to the onset of OAE 1a, in a highly restricted marine / lacustrine setting.

Keywords

Geochronology; Rhenium-Osmium; Barremian / Aptian boundary; Restricted marine

1. Introduction

Located in northeastern Brazil, the Araripe Basin, in the Borborema Province, is characterized by a Pre-Cambrian basement that exhibits a predominant northeast-southwest structural orientation. As a result, the architecture of the Araripe Basin is strongly characterized by horsts and grabens, that were formed in association with the rifting of Gondwana and the opening of the South Atlantic during the earliest Cretaceous (Hauterivian; Fig. 1; Matos, 1992; Ponte and Ponte Filho, 1996). The Araripe Basin comprises the Vale do Cariri, and the Chapada do Araripe regions that exhibit positive, tabular, and elongated E-W relief with sedimentary strata that gently dip to the west (Assine, 2007). Deposited into an intracratonic setting, the Paleozoic Cariri Formation represents the earliest sedimentation in the basin (Assine, 2007). Mesozoic successions comprise the pre-rift Cretaceous Neocomian Brejo Santo and Missão Velha formations, syn-rift Berriasian-Hauterivian Abaiara Formation, post-rift I Aptian-Albian Santana Group (Barbalha, Crato, Ipubi and Romualdo formations), and the post-rift II Albian-Cenomanian Araripe Group (Araripina and Exu formations; Fig. 2; Ponte and Ponte Filho, 1996; Batten, 2007; Assine, 2007; Scherer et al., 2014; Assine et al., 2014; Neumann and Assine, 2015; Fambrini et al., 2019).

The Araripe Basin has received significant attention, mainly because of its rich fossil content of the Santana Group (Crato and Romualdo formations) which have been utilized for paleoenvironmental, paleoclimatic, paleoecologic and paleogeographic reconstructions (Beurlen, 1964; Lima, 1978; Arai, 2012, 2014; Tomé et al., 2014; Sucerquia et al., 2015; Prado et al., 2015; Pereira et al., 2016; Field and Martill, 2017; Oliveira and Kellner, 2017). The Crato Formation includes one of the most critical terrestrial arthropod assemblages in the world due to the presence of primitive mayfly, dragonfly, earwig, grasshoppers, beetles, butterflies, spiders and scorpions (Martill et al., 2007). Ostracods, conchostracans and a rare caridean shrimp represent the crustaceans (Schweigert et al., 2007). Fossilized fish are dominated by *Dastilbe crandalli*, *Cladocyclus*, *Lepidotes* and *Araripelepidotes* (Davis and Martill, 1999), with *Vinctifer*, *Cladocyclus*, *Rhacolepis*, *Notelops*, *Mawsonia* and *Axelrodichthys* also being present in the Romualdo Formation. Further, well preserved wing membranes and wing fibres, claw sheaths, foot webs, and a heel pad of pterosaurs (*Arthurdactylus*, *Ludodactylus*, *Ingridia*, *Santanadactylus*, *Araripesaurus*, *Cearadactylus*, *Brasileodactylus*, *Anhanguera*, *Lacusovagus*) have been discovered from the Crato and

Romualdo formations (Martill and Unwin, 1989; Martill and Frey, 1998; Frey et al., 2003; Unwin and Martill, 2007; Witton, 2007), with additional dinosaurs (*Irritator*, *Angaturama*, *Santanaraptor* and *Mirischia*) being known in the Romualdo Formation (Kellner, 1996, 1999; Martill et al., 1996, 2000).

The age atributted to the whole ~~entire~~ Santana Group is indicated ~~characterized~~ by the *Cytheridea* spp. 201-208 Zone (NRT-011; Fig. 3; Coimbra et al., 2002). In contrast, ~~the diverse~~ palynomorphs reported to this group define two palynozones: the *Sergipea variverrucata* Zone (Barbalha and Crato formations) and the *Cicatricosisporites avnimelechi* Zone (Ipubi and Romualdo formations; Coimbra et al., 2002). These zones coincide with the interval between the Rio da Serra and Alagoas local stages (Berriasian to Aptian). Nevertheless, microfossils (e.g. *Pattersoncypris angulata*, *Pattersoncypris micropapillosa*, *Alicenula leguminella*) present in the Santana Group suggest that the Ipubi and Romualdo formations were deposited during the temporal framework of the Aptian and Albian stages (Regali, 1990; Coimbra et al., 2002). The presence of *Darwinula* in the ~~argillite~~ greenish mudstone that ~~infill~~ occurring filling fractures ~~in~~ crosscutting the evaporites overlying the black shales (both lithologies of the Ipubi Formation) and the presence of a single gyrogonite of Charophyta, has resulted in a *Darwinula-Charophyta* association for the Crato, Ipubi and Romualdo formations. Thus, this is considered to ~~which~~ constrain the age of the Ipubi Formation black shales to the Aptian and Albian stages (Fig. 3; Silva, 1975; Silva-Telles and Vianna, 1990; Neumann, 1999; Tomé et al., 2014).

Therefore, ~~our current knowledge of~~ until now the age ~~and evolution~~ of the Ipubi Formation is based solely on biostratigraphy, which constrains the deposition of the Ipubi Formation to a ~25 myr interval ~~that encompasses both~~ within the Aptian and Albian. To provide an improved understanding of the deposition timing of the Ipubi Formation and the entire Santana Group, and the evolution of the Araripe Basin, here we apply the rhenium-osmium isotope chronometer to the Ipubi Formation black shales and in turn show that the formation can be tied to the latest Barremian / earliest Aptian that was deposited in a lacustrine/highly restricted marine-influenced paleo-setting.

2. Geological aspects of the Ipubi Formation

The Ipubi Formation stratigraphically lies between the lacustrine limestones of the underlying Crato Formation and the marine calciferous sandstones and mudstones of the overlying Romualdo Formation (Ponte and Appi, 1990; Assine, 1992, 2007; Neumann and Cabrera, 1999; Assine et al., 2014; Neumann and Assine, 2015). Previous research has proposed that the post-rift phase I interval is represented by the Santana Formation, with the Crato, Ipubi and Romualdo being members, or even named differently (e.g., Santana Formation instead Romualdo Formation; Beurlen, 1971; Lima, 1979; Assine, 1994; 2007; Martill, 2007). More recently, it has been suggested that the Ipubi black shales and evaporites is a unit within the Crato Member (limestones) of the Santana Formation, with the different lithologies recording lateral variations that were deposited contemporaneously based on the order of marine evaporites and the absence of subaerial exposure and erosion (e.g., Bobco et al., 2017; Goldberg et al., 2019). However, regional lithology interdigitation of the Crato Formation with the Ipubi Formation evaporite is not observed (Bobco et al., 2017; Goldberg et al., 2019). Further, the proposal of interdigitation does not consider the presence of regionally recognized subaerial exposure that separates the Crato, Ipubi, and Romualdo units (Silva, 1986; Neumann and Cabrera, 1999; Assine et al., 2014; Neumann and Assine, 2015; Fabin et al., 2017). For example, the top of the Crato Formation is composed of calcrete formed under subaerial conditions (Neumann and Cabrera, 1999; Fabin et al., 2017), and the top of Ipubi Formation that is characterized by a subaerial exposure and erosion (karst surface) marked by large isolated columns and scattered depressions, pits and escarpments composed by clasts of gypsum, shale, fine-to-medium sandstone and quartz pebbles (Silva, 1986; Fabin et al., 2017). Lastly, based on mapping, stratigraphical correlation and sequence stratigraphy (well-known criteria considered to establish lithostratigraphic units according to Stratigraphic Guide by International Commission on Stratigraphy), the stratigraphic status of Ipubi and Santana units were changed to “Formation” and “Group”, respectively (Neumann and Cabrera,1999; Neumann and Assine, 2015), Based on the latter and our observation in both outcrop and boreholes we adopt the stratigraphic proposal of Neumann and Assine (2015).

In the post-rift phase I tectonic-sedimentary sequence of Araripe Basin, the Ipubi Formation comprises an evaporite (gypsum and anhydrite) interval 12-30 m thick associated with black shales of up to 5 m thick from its base, totaling 30 to 40 m in thickness (Neumann and Assine, 2015; Fabin et al., 2017). In the southwestern border region of the Araripe Basin, this formation directly overlies the Precambrian basement units (3.4 to 2.1 Ga; Silva et al., 1997; Fetter et al., 1999; Sato et al., 2012; Ancelmi, 2016; Martins, 2017; Vale, 2018). In contrast, in the northeastern region of the basin the Ipubi Formation overlies limestone of the Crato Formation or units of older (Early Cretaceous) tectonic-sedimentary phases of the basin (Neumann and Cabrera, 1999; Assine et al., 2014; Fabin et al., 2017). Concerning the representative area chose to sampling in this contribution, in the southwestern part of the basin, the Ipubi Formation black shales are characterized by dark to gray shales, mudstones, and carbonates, laminated, ostracode-rich, with pyrite and are bituminous (this study; Assine et al., 2014; Goldberg et al., 2019). Regionally, the upper portion of the black shale interval is interbedded with the gypsum lenses (< 10 cm wide) and bedding-parallel fibrous gypsum veins (Fabin et al., 2017). In the middle of the evaporite sequence, a sub-horizontal unconformity can regionally be observed in both the southwestern and northeastern borders of the basin (Souza Neto et al., 2013), which is filled by succession (40-60 cm wide) composed, from bottom to top, by plant fossil-bearing greenish mudstones, ostracd-conchostracan-rich laminated marls and thin black shales, and with gypsum-lenses (Souza Neto et al., 2013; Assine et al., 2014; Goldberg et al., 2019). Detailed petrographic observations and XRD analyses indicate that the black shales are predominantly composed of clay minerals (essentially illite-smectite), calcite, K-feldspar, quartz and minor celestite, apatite, and sulfides (Souza Neto et al., 2013; Nascimento Jr et al., 2016). The rocks are organic matter rich (TOC > 10 to 29 %; Souza et al., 2013; Castro et al., 2017), with both liquid chromatography data ((saturated + aromatic)/(polar) hydrocarbon ratios from 0.12 to 0.88; Lúcio et al., 2016a) and pyrolysis data indicating the shales to be hydrocarbon immature (T_{max} < 435° C and PI < 0.1; Castro et al., 2017) but endowed with a large gas potential (S_2 < 200 mg/g; Castro et al., 2017). Pristane/Phytane ratios of < 1 (Silva et al., 2014; Castro et al., 2017) and V/(V + Ni) ratios between 0.6 and 0.8 (Lúcio et al., 2016b) of the shales propose deposition under reducing conditions.

The presence of dynoflagellates (*Spinierites* and *Subtilisphaera*; Arai and Coimbra, 1990) and palynoforaminifers (organic linings and allied material; Lima, 1978; Arai, 2012; Goldberg et al., 2019), predominance of odd-to-even *n*-alkanes (Silva et al., 2014), and low organic phosphorus content (< 2 %; Souza Neto et al., 2013) in the black shales is interpreted to indicate deposition in a marine setting, which is supported by the sulphur isotope data ($\delta^{34}S$ = ~10 to 18 ‰; Bobco et al., 2017) of the overlying evaporite unit. However, a pure marine setting for Ipubi Formation black shales is not supported by the presence of non-marine ostracods (*Harbinia alta* and *Darwinula*; Antonietto et al., 2012; Tomé et al., 2014) and lacustrine facies (Assine, 2007; Assine et al., 2014). Based on the presence of evaporites, the Southern Australian sabkha environment has been proposed as a modern day analogue model for the paleogeography of the Ipubi Formation (Silva, 1988; Oliveira et al., 1979; Assine, 2007; Assine et al., 2014; Bobco et al., 2017; Fabin et al., 2017; Goldberg et al., 2019). being known as a shoreline with a restricted connection to the open ocean (Warren, 2016).

3. Sampling and analytical methods

Nine samples of black shales were collected from the Ipubi Formation in the southwestern portion of the Araripe Basin from the open pit Campevi mine in Gergelim County that excavates the evaporate of the Ipubi Formation (Fig. 2). The Ipubi Formation black shales occur stratigraphically below the evaporite sequence and are present beneath the quarry floor. To sample the formation, trenches in the quarry floor were dug about 1 m vertically beneath the surface exposure and ~4 m laterally from each other. The trenches were dug to expose a 1 m stratigraphic interval of the Ipubi Formation black shales (Fig. 4). All exposed surfaces showed black shales with variations in their facies (described below), were unweathered and care was taken to avoid zones of fractures and gypsum-veins and -lenses that were present in some trenches. The stratigraphic profile (Fig. 4) of the black shale unit comprises from bottom to top a 20 cm thick bituminous mudstone with an incipient laminar structure (~20 cm wide) that is overlain by a 30 cm interval of bituminous black shale exhibiting a millimeter to centimeter intercalated succession of light-coloured marls. The latter is overlain by 50 cm interval of bituminous laminated black shale that is fossiliferous (plants, preferentially preserved with a brown and phosphate-rich coating), with pyrite-bearing nodules (< 5 mm diameter), and gypsum-rich lenses (> 3 cm long). Samples were collected at a same deep position, about 1 m, predominantly from the mudstone and black shale interbedded marl horizons (see Table 1 for detail).

At the Laboratory of Geochemistry Applied to Petroleum at the Federal University of Pernambuco, the samples were washed with deionized water, then dried (at 60 °C for ~12 h) in an oven and powdered (~25 g) in an electric agate grinder (Pulverisette 7 classic line). The organic matter (OM %) and carbonate contents ($CaCO_3$ %) were obtained by weight-loss (at 360 °C for ~4 h and 1050 °C for ~1 h, respectively) and aluminium content (Al ppm) by Energy Dispersive X-ray Fluorescence (EDXRF), respectively (Table 1). The Al content was used to calculate the enrichment factor of both Re and ^{192}Os content in the organic-rich sampled horizon (Algeo and Maynard, 2004; Tribovillard et al., 2006; Table 1).

The Re and Os isotopic compositions and elemental abundances for the rock powders were determined at the Durham Geochemistry Center at Durham University. Approximately ~1 g of sample powder was digested with a mixed tracer (spike) solution of ^{190}Os and ^{185}Re in a Cr^{VI}–H_2SO_4 solution at 240 °C for ~48 h (cf. Selby and Creaser, 2003). The Cr^{VI}–H_2SO_4 dissolution media selectively liberates the hydrogenous Re and Os from the sediment limiting any detrital contribution (Selby and Creaser, 2003; Kendall et al., 2004). Rhenium and osmium were purified from the acid solution using solvent extraction, micro-distillation and anion chromatography methods. The purified Re and Os fractions were loaded onto Ni and Pt filaments, respectively (Selby et al., 2007), with the isotopic measurements conducted using negative thermal ionization mass spectrometry (Creaser et al., 1991) on a Thermo Scientific TRITON mass spectrometer via static Faraday collection for Re and ion-counting using a secondary electron multiplier in peak-hopping mode for Os in the Arthur Holmes Laboratory at Durham University.

The uncertainties for ^{187}Re/^{188}Os and ^{187}Os/^{188}Os was performed by error propagation incorporating uncertainties from the Re and Os mass spectrometer measurements, total blank abundances (Re = 12 ± 1 pg, Os = 0.08 ± 0.02 pg) and Os isotopic composition (^{187}Os/^{188}Os = 0.23 ± 0.01), spike calibrations, and reproducibility of standard Re and Os isotopic values. The Re-Os isotopic data, 2σ calculated uncertainties for ^{187}Re/^{188}Os and ^{187}Os/^{188}Os and the associated error correlation function (rho; Ludwig, 1980) are regressed using the beta version of Isochron program (Li et al., 2019) which incorporates the benchmark Isoplot algorithm (Ludwig, 2012) and the Monte Carlo sampling method for error propagation to yield a Re-Os age using the λ ^{187}Re constant of $1.666e^{-11} \pm 5.165e^{-14}$ a^{-1} (Smoliar et al., 1996).

In the beta version of Monte Carlo Isochron technique (Li et al., 2019), a prescribed number of isochrons (10^6) are created from the input data and their corresponding probability density function (analytical uncertainty of ^{187}Re/^{188}Os and ^{187}Os/^{188}Os values, and their error correlation, rho). The age and Os_i estimate for each iteration are crossed plotted yielding a probabilistic distribution that includes analytical uncertainty. Model uncertainties, those attributed to the isochron linear regression, are also calculated. In the Isoplot program (Ludwig, 2012), a Model 1 age implies that the assigned 2σ uncertainties and calculated error correlations are the only cause of the scatter in the data-points from the regression line; whereas a Model 2 best-fit assigns equal weight and zero error-correlations to each point; in contrast, a Model 3 age assumes that the scatter about the isochron line may be linked to both geological factors that produce variation in the initial $^{187}Os/^{188}Os$ values and the assigned analytical uncertainties. The isoplot program also yields the Mean Square of Weighted Deviates (MSWD), a measure of the deviation of the data points from the regression line that is strongly controlled by calculated uncertainties and error correlations.

4. Results

The sampled units from the Ipubi Formation black shales possess between 23.8 and 45.8 % of $CaCO_3$, 5.1 and 18.3 % of organic matter (OM), and 4802.9 and 64566.5 ppm of Al (Table 1). Black shale interbedded marl samples possess the highest $CaCO_3$ and lowest Al contents (Table 1). The total Re, total Os and ^{192}Os (best estimate of hydrogenous osmium) concentrations for the Ipubi Formation black shales sequence are 0.61-33.73 ppb, 26.8-273.5 ppt, and 8.6-76.6 ppt, respectively (Table 1). Both Re and Os are enriched, except for the Os abundance for sample TM07, compared to the upper continental crust (0.2-2 ppb Re and 30-50 ppt Os; Esser and Turekian, 1993; Sun et al., 2003). The enrichment factor (EF) value for Re and ^{192}Os ranges between 0.69 and 378.29, and 440.53 and 28062.1, respectively (Table 1). An enrichment factor greater than 1 is considered to indicate that the element is enriched relative to that of average shale, with an enrichment factor less than 1 being depleted (Tribovillard et al., 2006). Given this principle, only sample TM09 from Ipubi Formation black shale is depleted in Re, with all black shale interbedded marl samples exhibiting the highest level of enrichment in both Re and ^{192}Os (Table 1). In order to allow a direct comparison of hydrogenous Os concentrations in the different samples, the ^{192}Os abundance is used to avoid the addition of radiogenic ^{187}Os from ^{187}Re decay following deposition. A broad positive correlation exists between ^{192}Os (r = 0.75) and Re (r = 0.65) and OM elemental, and enrichment factor values with OM (Fig. 5), suggesting an uptake mechanism that is possibly linked to the abundance of organic matter (Georgiev et al., 2012; Rooney et al., 2012). Although, a correlation between OM and Re and ^{192}Os is not always observed (Rotich et al., 2020 and references therein). In case of the Ipubi Formation black shales, the broad relationship between OM and Re and ^{192}Os may also suggest that the samples were not affected by oxidative weathering, particularly as the Os_i values for Ipubi Formation black shales are positive (Table 1), which has been suggested to not indicate disturbance to the Re-Os system through oxidative weathering (Jaffe et al., 2002; Georgiev et al., 2012).

The $^{187}Re/^{188}Os$ (85.5 to 875.6) values positively correlate with their corresponding $^{187}Os/^{188}Os$ (1.922 to 3.757) compositions (Table 1). Regression of all the Re-Os isotope data using the Isoplot program (Ludwig, 2012) yields a Model 3 (discussed above) isochron age of 130.22 ± 12.57 (12.59 - bracketed value here and below includes uncertainty in the decay constant) Ma (n = 9; Mean Square of Weighted Deviates [MSWD] = 58.5), with an Os_i of 1.91 ± 0.11 (Fig. 6). An essentially identical age (130.2 ± 11.68 [11.69] Ma) and Os_i (1.91 ± 0.10) is determined from the beta version of the Isochron program, which incorporates a new approach that employs the Monte Carlo sampling method for error propagation (Li et al., 2019) and the benchmark Isoplot algorithm (Ludwig, 2012), except that the uncertainty in the age is slightly smaller, but the Monte Carlo approach highlights that 80% of the uncertainty relates to the model age calculation (Fig. 6). This uncertainty was also shown by the Re-Os data of organic-rich rocks of the Green River Formation, USA (Pietras et al., 2020) and East Coast Basin, New Zealand (Rotich et al., 2020).

5. Discussion

5.1 Re-Os isotopic systematics of the black shales from Ipubi Formation

The application of the Re-Os geochronometer has permitted the determination of accurate and precise depositional ages for lacustrine, fluvio-deltaic and marine organic-rich sedimentary rocks (e.g., Ravizza and Turekian, 1989; Cohen et al., 1999; Kendall et al., 2004; Selby and Creaser, 2005b; Kendall et al., 2006; Selby, 2007; Creaser et al., 2008: Kendall et al., 2009a; Selby et al., 2009; Yang et al., 2009; Poirier and Hillaire-Marcel, 2009, 2011; Baioumy et al., 2011; Cumming et al., 2012; Cumming et al., 2013; Tripathy and Singh, 2015; Xu et al., 2017; Pietras et al., 2020). Given the chalcophilic, siderophilic, and organophilic behaviour of Re and Os, they are found primarily in organic and sulphide phases. In organic-bearing sedimentary units Re and Os has been shown to be hydrogenous (derived from sequestration from the water column of the depositional setting) and primarily associated with/bound to organic matter (Ravizza and Turekian, 1989; Cohen et al., 1999; Selby and Creaser, 2003; Morford et al., 2005; Georgiev et al., 2011; Rooney et al., 2012).

As for other geochronological methods (e.g., Sm-Nd, Rb-Sr), the Re-Os chronometer utilizes the isochron technique to form a best-fit line of the $^{187}Re/^{188}Os$ vs $^{187}Os/^{188}Os$ data from an isochronous dataset. The degree of fit to the best fit line depends on the uncertainties associated with the Re and Os data (York, 1969) and are represented as a model classification (1, 2 or 3) that is based on the MSWD (reduced R^2 parameter; Ludwig, 2003). ~~A Model 1 best-fit of the data only takes into consideration the assigned uncertainties, whereas a Model 2 best-fit assigns equal weights and zero error-correlations to each point, and Model 3 best-fit presumes that the scatter is due to a combination of the assigned uncertainties and an unknown but normally distributed variation in the ordinate axis values.~~

Collectively both the Isoplot (Model 3 and high MSWD = ~58) and Monte Carlo (~80% of the uncertainty derived from the model age calculation) approaches highlight that all the Re-Os data do not fully satisfy the requirements to develop a precise isochron (Fig. 6A and 6B). The uncertainty in the Re-Os age (~12 myr) and the high MSWD value (~58, higher than the ideal value of ~1) determined from all the Re-Os data (n = 9) suggests that geological factors are the cause of the scatter of the data from the best-fit line. This could relate to the sample set possessing variable initial $^{187}Os/^{188}Os$ and/or post-depositional disturbance to the Re-Os systematics that could be related to fracturing and gypsum veining that were present in some trenches (Yang et al., 2009; Kendall et al., 2009b; Tripathy et al., 2014). A possible explanation for the high MSWD value for the best fit of all the Re-Os data for the nine samples from Ipubi Formation black shales is demonstrated by the range in the Os_i at 130 Ma (1.74 to 1.98; Table 1). For eight of the nine samples the calculated individual initial $^{187}Os/^{188}Os$ compositions at 130 Ma range from 1.86 to 1.98 (individual uncertainties are ± 0.02 - 0.03; Table 1). Sample TM09 yields a distinct initial $^{187}Os/^{188}Os$ value of 1.74 at 130 Ma. This sample exhibits the largest deviation from the 130 Ma best fit line of 8.3 %, whereas the other samples deviate between 0.3 and 2.1 %. Sample TM09 possesses an enrichment factor for Re of 0.69 suggesting that Re is depleted relative to the average upper continental crust in this sample, which may explain its deviation in the isochron or that the water column $^{187}Os/^{188}Os$ composition at the time of sediment deposition fluctuated across the sampled interval. Regression of the Re-Os data without sample TM09 yields a much more precise Isoplot Model 3 age of 124.7 ± 5.90 [5.93] Ma (initial $^{187}Os/^{188}Os$ = 1.97 ± 0.05, MSWD = 16.9) (Fig. 6C). This determined age is essentially identical to the Monte Carlo approach (124.7 ± 5.63 [5.66]; initial $^{187}Os/^{188}Os$ = 1.97 ± 0.05) which also highlights that the age uncertainty is now more controlled (30 %) by the analytical uncertainty in the data (Fig. 6D). Although this Re-Os age is more precise, scatter about the best-fit line is still evident from the MSWD value of ~17, and that uncertainties in the model age calculation control the overall uncertainty in the derived age. Sample TM05 exhibits the largest deviation (1.9 %) from the ~125 Ma line of best-fit, whereas the other samples deviate only between 0.1 and 0.9 %. This deviation is also highlighted by sample TM05 possessing a distinct initial $^{187}Os/^{188}Os$ value of 2.03 at 125 Ma, whereas the other samples (with the exception of TM09) yield an average initial $^{187}Os/^{188}Os$ value of 1.97 at 125 Ma (Table 1). The Re-Os data of this study suggests that samples TM05 and TM09 possess different Os_i compositions to that of the remaining sample set (Table 1). Regression of the Re-Os data without samples TM05 and TM09 (Fig. 6E) yields an Isoplot Model 3 age of 124.04 ± 4.88 [4.91] Ma (initial $^{187}Os/^{188}Os$ = 1.96 ± 0.05, MSWD = 6.6). Again, this calculated age is essentially identical to the Monte Carlo approach (123.99 ± 4.65 [4.68]; initial $^{187}Os/^{188}Os$ = 1.97 ± 0.05) and further shows that the age uncertainty is almost controlled equally between analytical and calculated model age uncertainties (Fig. 6F). Again, although this Re-Os age is more precise, scatter about the best-fit line is still evident from the MSWD value of 6.6 (still higher than the ideal value of ~1), and that uncertainties in the model age calculation control the overall uncertainty in the derived age. Sample TM06 exhibits the largest deviation from the linear regression (0.8 %; Fig. 6E), and exhibits a nominally more radiogenic initial $^{187}Os/^{188}Os$ composition (2.00 ± 0.02) in comparison to the remaining samples (TM01-04, TM07-08; Os_i = 1.95-1.98 ± 0.02 - 0.03 [average 1.96 ± 0.01 1 S.D.]; Table 1).

~~The isochron approach requires that the Re-Os systematics of the sample set meet the following criteria: (i) possess identical initial~~ $\cancel{^{187}Os/^{188}Os}$ ~~ratios, (ii) exhibit sufficient spread in~~ $\cancel{^{187}Re/^{188}Os}$ ~~ratios of at least a few hundred units, and (iii) the Re-Os systematics remain undisturbed (Cohen et al., 1999; Selby and Creaser, 2005a). Hence, the Ipubi Formation black shales show the~~ $\cancel{Os_i}$ ~~at 123 Ma range from 1.75 to 2.05 (Table 1).~~ The Re-Os data of this study shows that samples TM05, TM06 and TM09 possess different Os_i compositions to that of the remaining sample set (Table 1). Regression of the Re-Os data without TM05, TM06 and TM09 yields an Isoplot Model 1 age of 122.87 ± 1.53 [1.58] Ma (initial $^{187}Os/^{188}Os = 1.97 \pm 0.02$, MSWD = 1.04; Fig. 6G). Again, this calculated age is essentially identical to the Monte Carlo approach (122.61 ± 3.50 [3.52]; initial $^{187}Os/^{188}Os = 1.97 \pm 0.02$) and shows that the age uncertainty is more controlled (60 %) by the analytical uncertainties than the calculated model age uncertainties (Fig. 6H). Moreover, the greater uncertainty in the age derived by the Monte Carlo approach (± 3.50 [3.52]; Ma) further illustrates that a Model 1 Isoplot outcome underestimates the total age uncertainty arising from only considering analytical uncertainties (Li et al., 2019).

Given the isochronous behavior of the Re-Os data for six of the nine samples, which possess very similar initial $^{187}Os/^{188}Os$ composition, the moderate different initial $^{187}Os/^{188}Os$ values of TM05, TM06 and TM09 are considered to reflect changes in the $^{187}Os/^{188}Os$ composition of the water column during deposition rather than disturbance to the Re-Os systematics. Here, we consider the best estimate of the depositional age of the Ipubi Formation black shales to be 122.61 ± 3.50 [3.52] Ma.

The Re-Os age of ~123 Ma the Ipubi Formation black shales suggests that the studied samples were deposited during the latest Barremian/earliest Aptian. The new Re-Os age provides a significant improvement to the previous age determinations of Aptian to Albian (125 – 100.5 Ma) defined by relative dating age methods (Fig. 3; Coimbra et al., 2002; Tomé et al., 2014). Further, including the Re-Os age uncertainty, the Ipubi Formation black shale represents deposition just prior to the onset of OAE 1a (Arthur et al., 1990; Tejada et al., 2009; Jenkys, 2010). Moreover, this study suggests that, among the formations that constitute the Santana Group in the Araripe Basin, only the Romualdo (calciferous mudstone and sandstone) and Ipubi (black shales and evaporites) formations could be placed in the Aptian-Albian interval, whereas the Crato (calcareous rocks) and Barbalha (sandstone and mudstone) formations are older than the earliest Aptian (Fig. 2, 7). The latter age interval is emphasized by both palynological (e.g., *Afropollis jardinus*, *Classopollis classoides*) and ostracodal (e.g., *Damonella ultima*, *Damonella tinkoussouensis*) assemblages found in Santana Group (Coimbra et al., 2002; Neumann et al., 2003; Tomé et al., 2014; Nascimento et al., 2017), which are the same species found in Late Barremian successions worldwide (Hughes and McDougall, 1990; Bate, 1999; Gómez et al., 2001; Vallati, 2013).

5.2 ~~The beginning~~ Insights into the timing of the marine incursion in the Araripe Basin

The timing of the marine incursion in the Araripe Basin is extensively debated. Among the proposals, it is considered that the deposits of the Romualdo Formation (calciferous mudstone and sandstone) are the first records of a marine incursion in the Araripe Basin based on the presence of marine fossils (fishes, ostracods, gastropods, dynoflagellates and microforaminiferal linings; Lima, 1978; Arai and Coimbra, 1990; Maisey, 2000; Bruno and Hessel, 2006; Pereira et al., 2016) and facies associations (depositional sequences comprising transgressive and highstand system tracts; Assine, 2007; Rojas, 2009; Assine et al., 2014; Neumann and Assine, 2015; Custódio et al., 2017). Evidence for marine incursion during the deposition of the Ipubi Formation black shales is based on the occurrence of both dynoflagellates (*Spinierites* and *Subtilisphaera*; Arai and Coimbra, 1990) and palynoforaminifers (organic linings and allied material; Lima 1978; Arai, 2012; Goldberg et al., 2019), odd-to-even *n*-alkanes distribution (Silva et al., 2014), N/Vi ratios (0.13-0.49; Lúcio et al., 2016b) and Type II kerogen (Menezes, 2017). Further, some paleoceanographic/geographic reconstructions suggest that the Araripe Basin was, in part, based on the presence of microfossils (noted above), a significantly restricted NW-SE oriented marine basin that received incursion of the Western Tethys Sea via the northeastern Brazilian São Lúis and Parnáiba basins (Arai, 2014) (Fig. 8). In contrast, based on paleocurrent measurements in the Araripe and Tucano basins, a marine incursion into the Araripe Basin is also argued to have occurred from the south from the Proto South Atlantic (Assine et al., 2014; 2016).

The present-day open ocean $^{187}Os/^{188}Os$ composition of ~1.06 reflects the balance of inputs between radiogenic sources (average $^{187}Os/^{188}Os$ composition of the weathering of upper continental crust via riverine input, ~1.4) and non-radiogenic sources ($^{187}Os/^{188}Os$ ~0.13; cosmic dust, hydrothermal fluids, and weathering of mafic or ultramafic rocks; Esser and Turekian, 1993; Levasseur et al., 1998; Sharma et al., 1999; Woodhouse et al., 1999; Peucker-Ehrenbrink and Ravizza, 2000; Hannah et al., 2004). The current best estimate for the Late Barremian to Early Aptian (age of the Ipubi Formation black shales) open ocean $^{187}Os/^{188}Os$ composition is ~0.6 to 0.7 (Tejada et al., 2009; Bottini et al., 2012).

In lacustrine, fluvio-deltaic and restricted marine depositional settings the $^{187}Os/^{188}Os$ value of the water column can be highly radiogenic, e.g., ≥1.0 to 7.8 (Peucker-Ehrenbrink and Ravizza, 1996; Creaser et al., 2008; Poirier and Hillaire-Marcel, 2009, 2011; Baioumy et al., 2011; Cumming et al., 2012; Du Vivier et al., 2014; Tripathy et al., 2015; Xu et al., 2017; Pietras et al., 2020). Given the difference between the highly radiogenic $^{187}Os/^{188}Os$ value (1.75-2.05 at 123 Ma; Table 1) of the Ipubi Formation black shales to that of the Late Barremian to Early Aptian open ocean (~0.6 - 0.7) the initial $^{187}Os/^{188}Os$ data would suggest a predominantly continental source for Os to the Araripe Basin from the weathering of basin adjacent Proterozoic to Archean igneous, metaigneous and metasedimentary units (Silva et al., 1997; Fetter et al., 1999; Sato et al., 2012; Ancelmi, 2016; Martins, 2017; Vale, 2018). Therefore, based on our Os_i values (average of 1.97 without TM05, TM06 and TM09 samples), coupled with biostratigraphy, organic and inorganic geochemistry and paleoceanographic reconstructions outlined above, we propose that the water mass associated with the deposition of the Ipubi Formation black shales during the Barremian/Aptian boundary was highly restricted.~~ and, probably, would have received its marine influence from the western Tethyan Sea, as proposed by Arai (2014).~~

6. Conclusions

This study provides the first absolute time constraints for the Ipubi Formation black shales of the Santana Group at 123 ± 3.5 Ma. The age derived from Re-Os geochronology constrains deposition to the latest Barremian to the earliest Aptian, nominally prior to the onset of OAE 1a. The highly radiogenic initial $^{187}Os/^{188}Os$ composition (1.75 - 2.054) of the Ipubi Formation black shales coupled with widely recognized paleontological, geochemical evidence, together with paleoceanographic reconstructions, suggests that the Araripe Basin was a highly restricted water mass that was also marine influenced ~~and would have received its marine influence from the western Tethys Sea~~. The latter is in temporal agreement with a global eustasy rise during the Mid Cretaceous.

Acknowledgements

We gratefully acknowledge Petrobras (Agreement Nº 25, Cooperation term 0050.0023165.06.4) and PRH-26 (Human Resources Program of the AnP: process number 48610.013803/2009-19) for research funding. TL and JASN are grateful to the mining engineer Flávia Bastos from Campevi Mine for mine access and assistance during the sampling, and to Dr. Juliana Marques Charão for advices concerning sampling. JASN is also grateful to CNPq for his research grant (process number 312.275/2017-0). DS acknowledges the TOTAL Endowment Fund and the Dida Scholarship (CUG Wuhan) and Antonia Hoffman, Geoff Nowell, and Chris Ottley for analytical support.

References

Algeo, T.J., Maynard, J.B., 2004. Trace-element behavior and redox facies in core shales of Upper Pennsylvanian Kansas-type cyclothems. Chemical Geology 206, 289-318. https://doi.org/10.1016/j.chemgeo.2003.12.009

Ancelmi, M.F., 2016. Geocronologia e geoquímica das rochas arqueanas do Complexo Granjeiro, Província da Borborema (PhD thesis). Universidade Estadual de Campinas, 159 pp. http://repositorio.unicamp.br/handle/REPOSIP/330571

Antonietto, L.S., Gobbo, S.R., Carmo, D.A., Assine, M.L., Fernandes, M.A.M.C.C., Lima, J.E., 2012. Taxonomy, Ontogeny and Paleoecology of Two Species of Harbinia TSAO, 1959 (Crustacea, Ostracoda) from the Santana Formation, Lower Cretaceous, Northeastern Brazil. Journal of Paleontology 86, 659-668. http://dx.doi.org/10.1666/11-012R.1

Arai M., 2012. Evidência micropaleontológica da ingressão marinha aptiana (pré-evaporítica) na Bacia do Araripe, Nordeste do Brasil. 46° Congresso Brasileiro de Geologia, Santos, Brasil. https://www.researchgate.net/publication/301302246_Evidencia_micropaleontologica_da_ingressao_marinha_aptiana_pre-evaporitica_na_Bacia_do_Araripe_Nordeste_do_Brasil

Arai M., Coimbra J.C., 1990. Análise paleoecológica do registro das primeiras ingressões marinhas na Formação Santana (Cretáceo Inferior da Chapada do Araripe). 1º Simpósio da Bacia do Araripe e Bacias Interiores do Nordeste. https://www.researchgate.net/publication/285667590_Analise_paleoecologica_do_regis tro_das_primeiras_ingressoes_marinhas_na_Formacao_Santana_Cretaceo_Inferior_da_Chapada_do_Araripe

Arai, M., 2014. Aptian/Albian (Early Cretaceous) paleogeography of the South Atlantic: A paleontological perspective. Brazilian Journal of Geology 44 (2), 339-350. http://dx.doi.org/10.5327/Z2317-4889201400020012

Arthur M.A., Brumsack HJ., Jenkyns H.C., Schlanger S.O., 1990. Stratigraphy, Geochemistry, and Paleoceanography of Organic Carbon-Rich Cretaceous Sequences. In: Ginsburg R.N., Beaudoin B. (Eds.), Cretaceous Resources, Events and Rhythms. NATO ASI Series (Series C: Mathematical and Physical Sciences), 304. Springer, Dordrecht, 75-119. https://doi.org/10.1007/978-94-015-6861-6_6

Assine, M.L., 1992. Análise estratigráfica da Bacia do Araripe, nordeste do Brasil. Revista Brasileira de Geociências 22, 289-300. http://dx.doi.org/10.25249/0375-7536.1992289300

Assine, M.L., 2007. Bacia do Araripe. Boletim de Geociências da Petrobras 5, 371-389. https://www.researchgate.net/publication/279556073_Araripe_basin_Bacia_do_Araripe

Assine, M.L., Perinotto, J.A.J., Custódio, M.A., Neumann, V.H., Varejão, F.G., Mescolotti, P.C., 2014. Sequências deposicionais do Andar Alagoas da Bacia do Araripe, Nordeste do Brasil. Boletim de Geociências da Petrobras 22 (1), 3-28. https://www.researchgate.net/publication/311680092_Sequencias_Deposicionais_do_Andar_Alagoas_Aptiano_superior_da_Bacia_do_Araripe_Nordeste_do_Brasil

Baioumy, H.M., Eglinton, L.B., Peucker-Ehrenbrink, B., 2011. Rhenium-osmium isotope and platinum group element systematics of marine vs. non-marine organic-rich sediments and coals from Egypt. Chemical Geology 285, 70-81. https://doi.org/10.1016/j.chemgeo.2011.02.026

Bate, R.H., 1999. Non-marine ostracod assemblages of the Pre-salt rift basins of West Africa and their role in sequence stratigraphy. In: Cameron, N.R., Bate, R.H., Clure, V.S. (Eds.), The Oil and Gas Habitats of the South Atlantic. Geological Society of London. Special publication, 283-292. http://dx.doi.org/10.1144/GSL.SP.1999.153.01.17

Batten, D., 2007. Spores and pollen from the Crato Formation: Biostratigraphic and palaeoenvironmental implications. In: Martill, D.M., Bechly, G., Loveridge, R. (Eds.), The Crato Fossil Beds of Brazil: Window into an Ancient World. Cambridge: Cambridge University Press, 566-574. https://doi.org/10.1017/CBO9780511535512.021

Beurlen, K., 1964. As espécies dos Cassiopinae, nova subfamília dos Turriteliidae, no Cretáceo do Brasil. Arquivo de Geologia [UFPE] 5, 1-43. https://www.researchgate.net/publication/285317467_As_especies_dos_Cassiopinae_nova_subfamilia_dos_Turritellidae_no_Cretaceo_do_Brasil

Beurlen, K., 1971. Bacias sedimentares do Bloco Brasileiro. Estudos Sedimentológicos 1(2), 9-31.

Bobco, F.E.R., Goldberg, K., Bardola, T.P., 2017. Modelo deposicional do Membro Ipubi (Bacia do Araripe, nordeste do Brasil) a partir da caracterização faciológica, petrográfica e isotópica dos evaporitos. Pesquisas em Geociências 44(3), 431-451. https://doi.org/10.22456/1807-9806.83267

Bottini, C., Cohen, A.S., Erba, E., Jenkyns, H.C., Coe, A.L., 2012. Osmium-isotope evidence for volcanism, weathering, and ocean mixing during the early Aptian OAE 1a. Geology 40(7), 583-586. https://dx.doi.org/10.1130/G33140.1

Bruno, A.P.S., Hessel, M.H., 2006. Registros paleontológicos do cretáceo marinho na Bacia do Araripe. Estudos Geológicos 16 (1), 30-49. https://www3.ufpe.br/estudosgeologicos/paginas/edicoes/2006161/2006161t03.pdf

Castro, R.G., Silva-Santos, T.L., Fambrini, G.L., Souza Neto, J.A., Pereira, R., 2017. Caracterização geoquímica da matéria orgânica dos folhelhos betuminosos na Formação Ipubi, Bacia do Araripe, NE Brasil. Geochimica Brasiliensis 31 (1), 11-27. http://dx.doi.org/10.21715/GB2358-2812.2017301011

Cohen, A.S., Coe, A.L., Bartlett, J.M., Hawkesworth, C.J., 1999. Precise Re-Os ages of organic-rich mudrocks and the Os isotope composition of Jurassic seawater. Earth and Planetary Science Letters 167, 159-173. https://doi.org/10.1016/S0012-821X(99)00026-6

Coimbra, J.C., Arai, M., Carreño, A.L., 2002. Biostratigraphy of Lower Cretaceous Microfossils from the Araripe Basin, northeastern Brazil. Geobios 35, 687-698. https://doi.org/10.1016/S0016-6995(02)00082-7

Creaser, R., Szatmari, P., Milani, E.J., 2008. Extending Re-Os shale geochronology to lacustrine depositional systems: A case study from the major hydrocarbon source rocks of the Brazilian Mesozoic marginal basins. 33rd International Geological Congress, Oslo.

Creaser, R.A., Papanastassiou, D.A., Wasserburg, G.J., 1991. Negative thermal ion mass spectrometry of osmium, rhenium and iridium. Geochimica et Cosmochimica Acta 55, 397-401. https://doi.org/10.1016/0016-7037(91)90427-7

Cumming, V.M., Poulton, S.W., Rooney, A.D., Selby, D., 2013. Anoxia in the terrestrial environment during the late Mesoproterozoic. Geology 41 (5) 583–586. https://doi.org/10.1130/G34299.1

Cumming, V.M., Selby, D., Lillis, P.G., 2012. Re-Os geochronology of the lacustrine Green River Formation: Insights into direct depositional dating of lacustrine successions, Re-Os systematics and paleocontinental weathering. Earth and Planetary Science Letters 359-360, 194-205. https://doi.org/10.1016/j.epsl.2012.10.012

Custódio, M.A., Quaglio, F., Warren, L.V., Simões, M.G., Fürsich, F.T., Perinotto, J.A.J., Assine, M.L., 2017. The transgressive-regressive cycle of the Romualdo Formation (Araripe Basin): Sedimentary archive of the Early Cretaceous marine ingression in the interior of northeast Brazil. Sedimentary Geology 359, 1-15. https://doi.org/10.1016/j.sedgeo.2017.07.010

Davis, S.P; Martill, M., 1999. The gonorynchiform fish *Dastilbe* from the Lower Cretaceous of Brazil. Palaeontology 42 (4), 715-740. https://doi.org/10.1111/1475-4983.00094

Du Vivier, A., Selby, D., Sageman, B., Jarvis, I., Grocke, D., Voigt, S., 2014. Marine $^{187}Os/^{188}Os$ isotope stratigraphy reveals the interaction of volcanism and ocean circulation during Oceanic Anoxic Event 2. Earth and Planetary Science Letters 389, 23-33. https://doi.org/10.1016/j.epsl.2013.12.024

Esser, B.K., Turekian, K.K., 1993. The osmium isotopic composition of the continental crust. Geochimica et Cosmochimica Acta 57, 3093-3104. https://doi.org/10.1016/0016-7037(93)90296-9

Fabin, C.E., Correia Filho, O.J., Alencar, M.L., Barbosa, J.A., Miranda, T.S., Neumann, V.H., Gomes, I.F., Santana, F.R., 2018. Stratigraphic Relations of the Ipubi Formation: Siliciclastic-Evaporitic Succession of the Araripe Basin. Anais da Academia Brasileira de Ciências 90(2), 2049-2071. https://doi.org/10.1590/0001-3765201820170526

Fambrini, G.L., Silvestre, D.C., Menezes-Filho, J.A.B., Costa, I.C., Neumann, V.H.M.L., 2019. Architectural and facies characterization of the Aptian fluvial Barbalha Formation, Araripe Basin, NE Brazil. Geological Society, London, Special Publications 488, 119-150. https://doi.org/10.1144/SP488-2017-275

Fetter, A.H., Van Schmus, W.R, Santos, T.J.S., Nogueira Neto, J.A., Arthaud, M.H. 2000. U-Pb and Sm-Nd geochronological constraints on the crustal evolution and basement architecture of Ceará State, NW Borborema Province, NE Brazil: implications for the existence of the Paleoproterozoic Supercontinent "Atlantica". Revista Brasileira de Geociências 30(1), 102-106. http://www.ppegeo.igc.usp.br/index.php/rbg/article/view/10928

Field, G.J., Martill, D.M., 2017. Unusual soft tissue preservation in the Early Cretaceous (Aptian) crocodile cf. *Susisuchus* from the Crato Formation of north east Brazil. Cretaceous Research 75, 179-192. https://doi.org/10.1016/j.cretres.2017.04.001

Frey, E., Martill, D.M., Buchy, M.C., 2003. A new crested ornithocheirid from the Lower Cretaceous of northeastern Brazil and the unusual death of an unusual pterosaur. In: Buffetaut, E., Mazin, J.M. (Eds.), Evolution and Palaeobiology of Pterosaurs 217. Geological Society, London, Special Publications, 55-63. https://doi.org/10.1144/GSL.SP.2003.217.01.05

Georgiev, S., Stein, H.J., Hannah, J.L., Bingen, B., Weiss, H.M., Piasecki, S., 2011. Hot acidic Late Permian seas stifle life in record time. Earth and Planetary Science Letters 310, 389–400. https://doi.org/10.1016/j.epsl.2011.08.010

Georgiev S., Stein H., Hannah J., Weiss H., Bingen B., Xu G., Rein E., Hatlø V., Løseth H., Nali M., Piasecki S., 2012. Chemical signals for oxidative weathering predict Re–Os isochroneity in black shales, East Greenland. Chemical Geology 324–325, 108–121. https://dx.doi.org/10.1016/j.chemgeo.2012.01.003

Goldberg, K., Premaor, E., Bardola, T., Souza, P.A., 2019. Aptian marine ingression in the Araripe Basin: Implications for paleogeographic reconstruction and evaporite accumulation. Marine and Petroleum Geology 107, 214-221. https://doi.org/10.1016/j.marpetgeo.2019.05.011

Gómez, B., Martín-Closas, C., Méon, H., Thévenard, F., Barale, G., 2001. Plant taphonomy and palaeoecology in the lacustrine Uña delta (Late Barremian, Iberian Ranges, Spain). Palaeogeography, Palaeoclimatology, Palaeoecology 170, 133-148. https://doi.org/10.1016/S0031-0182(01)00232-2

Hannah, J.L., Bekker, A., Stein, H.J., Markey, R.J., Holland, H.D., 2004. Primitive Os and 2316 Ma age for marine shale: implications for Paleoproterozoic glacial events and the rise of atmospheric oxygen. Earth and Planetary Science Letters 225, 43–52. https://doi.org/10.1016/j.epsl.2004.06.013

Hughes, N.F., McDougall, A.B., 1990. Barremian-Aptian angiospermid pollen records from southern England. Review of Palaeobotany and Palynology 65, 145-151. https://doi.org/10.1016/0034-6667(90)90065-Q

Jaffe, L.A., Peucker-Ehrenbrink, B., Petsch, S.T., 2002. Mobility of rhenium, platinum group elements and organic carbon during black shale weathering. Earth and Planetary Science Letter 198, 339–353. https://doi.org/10.1016/S0012-821X(02)00526-5

Jenkyns, H.C., 2010. Geochemistry of oceanic anoxic events. Geochemistry, Geophysics, Geosystems 11(3), 1-30. https://doi.org/10.1029/2009GC002788

Kellner, A.W.A., 1996. Remarks on Brazilian dinosaurs. Memoirs of the Queensland Museum 39 (3), 611-626. https://www.researchgate.net/publication/285026172_Remarks_on_Brazilian_dinosaurs

Kellner, A.W.A., 1999. Short note on a new dinosaur (Theropoda, Coelurosauria) from the Santana Formation (Romualdo Member, Albian), northeastern Brazil. Boletim do Museu Nacional, Geologia 49, 1-8. https://www.researchgate.net/publication/284618038_Short_Note_on_a_new_dinosaur_

Theropoda_Coelurosauria_from_the_Santana_Formation_Romualdo_Member_Albian_northeastern_Brazil

Kendall B., Creaser R.A., and Selby D., 2006. Re-Os geochronology of postglacial black shales in Australia: Constraints on the timing of “Sturtian” glaciation. Geology 34, 729-732. https://doi.org/10.1130/G22775.1

Kendall, B., Creaser, R.A., Calver, C.R., Raub, T.D., Evans, D.A.D., 2009a. Correlation of sturtian diamictite successions in southern Australia and northwestern Tasmania by Re-Os black shale geochronology and the ambiguity of “Sturtian”-type diamictite-cap carbonate pairs as chronostratigraphic marker horizons. Precambrian Research 172, 301-310. http://dx.doi.org/10.1016/j.precamres.2009.05.001

Kendall, B., Creaser, R.A., Gordon, G.W., Anbar, A.D., 2009b. Re-Os and Mo isotope systematics of black shales from the Middle Proterozoic Velkerri and Wollogorang formations, McArthur Basin, northern Australia. Geochimica et Cosmochimica Acta 73, 2534-2558. https://doi.org/10.1016/j.gca.2009.02.013

Kendall, B.S., Creaser, R.A., Ross, G.M., Selby, D., 2004. Constraints on the timing of Marinoan “Snowball Earth” glaciation by ^{187}Re-^{187}Os dating of a Neoproterozoic post-glacial black shale in western Canada. Earth and Planetary Science Letters 222, 729-740. https://doi.org/10.1016/j.epsl.2004.04.004

Levasseur, S., Birck, J., Allegre, C.J., 1998. Direct measurement of femtomoles of osmium and the ^{187}Os/^{186}Os ratio in seawater. Science 282, 272-274. https://doi.org/10.1126/science.282.5387.272

Li, Y., Zhang, S., Hobbs, R., Caiado, C., Sprosson, A.D., Selby, D., Rooney, A.D., 2019. Monte Carlo sampling for error propagation in linear regression and applications in isochron geochronology. Science Bulletin 64 (3), 189-197. https://doi.org/10.1016/j.scib.2018.12.019

Lima, M.R., 1978. Palinologia da Formação Santana (Cretáceo do Nordeste do Brasil) (PhD thesis). São Paulo University, 335 pp. https://doi.org/10.11606/T.44.1978.tde-16112015-153709

Lima, M.R., 1979. Considerações sobre a subdivisão estratigráfica da Formação Santana Cretáceo do Nordeste do Brasil. Revista Brasileira de Geociências 9(2), 116-121. http://www.ppegeo.igc.usp.br/index.php/rbg/article/view/12366

Lúcio, T., Almeida, C.M.T., Pacheco Filho, J.G.A., Araújo, J.C.M., Souza Neto, J.A., Pereira, R., 2016a. Grau de maturação dos hidrocarbonetos dos folhelhos pirobetuminosos da Formação Ipubi, Bacia do Araripe: Um estudo integrado de termogravimetria, cromatografia e espectroscopia na região do infravermelho. Estudos Geológicos 26(1), 81-97. https://doi.org/10.18190/1980-8208/estudosgeologicos.v26n1p81-97

Lúcio, T., Moura, W.A.L., Araújo, J.C.M., França, E., Souza Neto, J.A., Pereira, R., 2016b. Geoquímica da Formação Ipubi, Bacia do Araripe, PE: aspectos da mineralogia, paleoclima, paleoambiente e paleossalinidade. XIII Congresso de Geoquímica dos Países de Língua Portuguesa / I Workshop de Geomatemática nas Ciências da Terra, Fortaleza, Brasil. https://www.researchgate.net/publication/317225587_Geoquimica_da_Formacao_Ipubi_Bacia_do_Araripe_PE_aspectos_da_Mineralogia_Paleoclima_Paleoambiente_e_Paleossalinidade

Ludwig, K.R., 1980. Calculation of uncertainties of U-Pb isotope data. Earth and Planetary Science Letter 46, 212-220. https://doi.org/10.1016/0012-821X(80)90007-2

Ludwig, K.R., 2003. User's manual for Isoplot 3.00: A geochronological toolkit for Microsoft Excel. Special publication / Berkeley Geochronology Center 4. https://www.researchgate.net/publication/301951506_User%27s_Manual_for_IsoplotEx_rev_300_A_Geochronological_Toolkit_for_Microsoft_Excel

Ludwig, K.R., 2012. Isoplot, version 3.75: A geochronological Toolkit for Microsoft Excel. Berkeley Geochronology Center Special Publication No. 5. http://www.bgc.org/isoplot_etc/isoplot/Isoplot3_75-4_15manual.pdf

Maisey, J.G., 2000. Continental break-up and the distribution of fishes in Western Gondwana during the Early Cretaceous. Cretaceous Research 21, 281-314. https://doi.org/10.1006/cres.1999.0195

Martil, D.M., Unwin, D.M., 1989. Exceptionally well preserved pterosaur wing membrane from the Cretaceous of Brazil. Nature 340, 138-140. https://doi.org/10.1038/340138a0

Martill, D.M. (Ed.), 1996. Fossils of the Santana and Crato Formations, Brazil. Palaeontological Association Field Guides to Fossils 5, 160 pp.

Martill, D.M., 2007. The age of the Cretaceous Santana Formation fossil Konservat Lagerstätte of north-east Brazil: A historical review and an appraisal of the biochronostratigraphic utility of its palaeobiota. Cretaceous Research 28, 895-920. https://doi.org/10.1016/j.cretres.2007.01.002

Martill, D.M., Bechly, G. and Loveridge, R.F. (Eds.), 2007. The Crato Fossil Beds of Brazil: Window into an Ancient World. Cambridge University Press, Cambridge, 625 pp. https://doi.org/10.1017/CBO9780511535512

Martill, D.M., Cruickshank, A. R. I., Frey, E., Small P.G., Clarke M., 1996. A new crested maniraptoran dinosaur from the Santana Formation (Lower Cretaceous) of Brazil. Journal of the Geological Society 153, 5-8. https://doi.org/0.1144/gsjgs.153.1.0005

Martill, D.M., Frey, E., 1998. A new pterosaur Lagerstätte in N.E. Brazil (Crato Formation; Aptian, Lower Cretaceous): Preliminary observations. Oryctos 1, 79-85. https://www.researchgate.net/publication/288089527_A_new_pterosaur_Lagerstatte_in_N_E_Brazil_Crato_Formation_Aptian_Lower_Cretaceous_Preliminary_observations

Martill, D.M., Frey, E., Sues, H.D., Cruickshank, A.R.I, 2000. Skeletal remains of a small theropod dinosaur with associated soft structures from the Lower Cretaceous Santana Formation of northeastern Brazil. Canadian Journal of Earth Sciences 37 (6), 891-900. https://doi.org/10.1139/e00-001

Martins, D.T., 2017. Evolução tectônica das rochas encaixantes das Formações Ferríferas Bandadas de Manga Velha-PI, Província Borborema (Unpbl. PhD thesis). Universidade Federal do Ceará, 86 pp.

Matos R.M.D., 1999. History of the northeast Brazilian rift system: kinematic implications for the break-up between Brazil and West Africa. In: Cameron, N.R., Bate, R.H., Clure, V.S. (Eds.), The Oil and Gas Habitats of the South Atlantic. Geological

Society, London, Special Publications 153, 55-73. https://doi.org/10.1144/GSL.SP.1999.153.01.04

Matos, R.M.D., 1992. The Northeast Brazilian Rift System. Tectonics 11, 766-791. https://doi.org/10.1029/91TC03092

Medeiros V.C., 2004. Evolução geodinâmica e condicionamento estrutural dos terrenos Piancó-Alto Brígida e Alto Pajeú, Domínio da Zona Transversal, NE do Brasil (PhD thesis). Federal University of Rio Grande do Norte, 200 pp. http://rigeo.cprm.gov.br/jspui/handle/doc/105

Menezes, J.D.O., 2017. Geoquímica e petrografia orgânica da Formação Santana, Bacia do Araripe, Nordeste do Brasil (PhD thesis). Federal University of Rio Grande do Sul, 75 pp. http://hdl.handle.net/10183/156391

Morford J.L., Emerson S.R., Breckel E.J., Hyun Kim S., 2005. Diagenesis of oxyanions (V, U, Re and Mo) in pore waters and sediments from a continental margin. Geochimica Cosmochimica et Acta 69, 5021-5032. https://doi.org/10.1016/j.gca.2005.05.015

Morford, J.L., Emerson, S., 1999. The geochemistry of redox sensitive trace metals in sediments. Geochimica et Cosmochimica Acta 63, 1735-1750. https://doi.org/10.1016/S0016-7037(99)00126-X

Nascimento Jr, D.R., da Silva Filho, W.F., Freire Jr, J.G., dos Santos, F.H., 2016. Syngenetic and diagenetic features of evaporite-lutite successions of the Ipubi Formation, Araripe Basin, Santana do Cariri, NE Brazil. Journal of South American Earth Sciences 72, 315-327. https://doi.org/10.1016/j.jsames.2016.10.001

Nascimento, L.R.S.L., Tome, M.E.T.R., Barreto, A.M.F., Oliveira, D.H., Neumann, V.H.M.L., 2017. Diagnóstico palinoflorístico do poço 2-JNS-01PE, Cretáceo Inferior, Bacia do Jatobá, Nordeste do Brasil. Estudo Geológicos 27(1), 118-134. https:// 10.18190/1980-8208/estudosgeologicos.v27n1p118-134

Neumann, V.H., Assine, M.L., 2015. Stratigraphic proposal to the post-rift I tectonic-sedimentary sequence of Araripe Basin, Northeastern Brazil. 2nd International Congress on Stratigraphy, Graz, Austria.

Neumann, V.H., Borrego, A.G., Cabrera, L., Dino, R., 2003. Organic matter composition and distribution through the Aptian–Albian lacustrine sequences of the Araripe Basin, northeastern Brazil. International Journal of Coal Geology 54, 21-40. https://doi.org/10.1016/S0166-5162(03)00018-1

Neumann, V.H., Cabrera, L., 1999. Una nueva propuesta estratigráfica para la tectonosecuencia post-rifte de la Cuenca de Araripe, noreste de Brasil. 5º Simpósio sobre o Cretáceo do Brasil / 1º Simpósio sobre el Cretácico de América del Sur, Serra Negra. Brasil. https://www.researchgate.net/publication/285885346_Una_nueva_propuesta_estratigrafica_para_la_tectonosecuencia_post-rifte_de_la_cuenca_de_Araripe_noreste_de_Brasil

Neumann, V.H.M.L., 1999. Estratigrafia, sedimentologia, geoquímica y diagénesis de los sistemas lacustres Aptienses-Albienses de la Cuenca de Araripe (Noreste de Brasil) (Unpbl. PhD thesis). Universitat de Barcelona, 233 pp.

Oliveira, A.A., Brito, A.L.F., Santos, M.E.C.M., Carvalho, M.S.S., 1979. Projeto Chapada Do Araripe. DNPM/CPRM Final Report 1, 123.

Oliveira, G.R., Kellner, A.W.A., 2017. Rare hatchling specimens of *Araripemys* Price, 1973 (Testudines, Pelomedusoides, Araripemydidae) from the Crato Formation, Araripe Basin. Journal of South American Earth Sciences 79, 137-142. https://doi.org/10.1016/j.jsames.2017.07.014

Pereira, P.A., Cassab, R.D.C.T., Barreto, A.M.F., 2016. Cassiopidae gastropods, influence of Tethys Sea of the Romualdo Formation (Aptian-Albian), Araripe Basin, Brazil. Journal of South American Earth Sciences 70, 211-223. https://doi.org/10.1016/j.jsames.2016.05.005

Peucker-Ehrenbrink, B., Ravizza, G., 1996. Continental runoff of osmium into the Baltic Sea. Geology 24 (4), 327-330. https://doi.org/10.1130/0091-7613(1996)024%3C0327:CROOIT%3E2.3.CO;2

Peucker-Ehrenbrink, B., Ravizza, G., 2000. The marine osmium isotope record. Terra Nova 12, 205-219. https://doi.org/10.1046/j.1365-3121.2000.00295.x

Pietras, J.T., Selby, D., Brembs, R., Dennett, A., 2020. Tracking drainage basin evolution, continental tectonics, and climate change: Implications from osmium isotopes of lacustrine systems. Palaeogeography, Palaeoclimatology, Palaeoecology 537, 109471. https://doi.org/10.1016/j.palaeo.2019.109471

Poirier, A., Hillaire-Marcel, C., 2011. Improved Os-isotope stratigraphy of the Arctic Ocean. Geophysical Research Letter 38, 1-6. https://doi.org/10.1029/2011GL047953

Poirier, A., Hillaire□Marcel., C., 2009. Os□isotope insights into major environmental changes of the Arctic Ocean during the Cenozoic. Geophysical Research Letter 36, 1-5. doi:10.1029/2009GL037422

Ponte, F.C., Appi, C.J., 1990. Proposta de revisão da coluna litoestratigráfica da Bacia do Araripe. 36º Congresso Brasileiro de Geologia, Natal, Brasil, 211-226.

Ponte, F.C., Ponte Filho, F.C., 1996. Estrutura Geológica e Evolução Tectônica da Bacia do Araripe. DNPM, Recife, 98 pp.

Prado, L.A.C., Pereira, P.A., Sales, A.M.F., Barreto, A.M.F., 2015. Taphonomic and paleoenvironmental considerations for the concentrations of macroinvertebrate fossils in the Romualdo Member, Santana Formation, Late Aptian-Early Albian, Araripe Basin, Araripina, NE, Brazil. Journal of South American Earth Sciences 62, 218-228. https://doi.org/10.1016/j.jsames.2015.06.005

Ravizza, G., Turekian, K.K., 1989. Application of the ^{187}Re-^{187}Os system to black shale geochronometry. Geochimica et Cosmochimica Acta 53, 3257-3262. https://doi.org/10.1016/0016-7037(89)90105-1

Regali, M.S.P., 1990. A idade dos evaporitos da plataforma continental do Ceará, Brasil, e sua relação com os outros evaporitos das bacias nordestinas. Boletim do IG-USP 7, 139-143. https://doi.org/10.11606/issn.2317-8078.v0i7p139-143

Rojas, F.E.M., 2009. Estratigrafia de sequências do intervalo Aptiano ao Albiano na Bacia do Araripe, NE do Brasil (Masters dissertation). Federal University of Rio Grande do Norte, 122 pp. http://dx.doi.org/10.1590/S0102-261X2010000100011

Rooney, A.D., Selby, D., Lewan, M.D., Lillis, P.G., Houzay, J.P., 2012. Evaluating Re-Os systematics in organic-rich sedimentary rocks in response to petroleum generation using hydrous pyrolysis experiments. Geochimica et Cosmochimica Acta 77, 275-291. https://doi.org/10.1016/j.gca.2011.11.006

Rotich, E.K., Handler, M.R., Naeher, S., Selby, D., Hollis, C.J., Sykes, R., 2020. Re-Os geochronology and isotope systematics, and organic and sulfur geochemistry of the middle–late Paleocene Waipawa Formation, New Zealand: Insights into early Paleogene seawater Os isotope composition. Chemical Geology 536, 1-18. https://doi.org/10.1016/j.chemgeo.2020.119473

Sato, E.N, Almeida, T.I.R., Basei, A.S., 2012. Idades U-Pb em zircões das rochas encaixantes das formações ferríferas do distrito de Curral Novo do Piauí, Brasil. 34th International Geological Congress (IGC), Austrália.

Scherer, C.M.S., Jardim de Sá, E.F., Córdoba, V.C., Sousa, D.C., Aquino, M.M., Cardoso, F.M.C., 2014. Tectono-stratigraphic evolution of the Upper Jurassic-Neocomian rift succession, Araripe Basin, Northeast Brazil. Journal of South American Earth Sciences 49, 106-122. https://doi.org/10.1016/j.jsames.2013.10.007

Schweigert, G., Martill, D., Williams, M., 2007. Crustacea of the Crato Formation. In: Martill, D.M., Bechly, G., Loveridge, R. (Eds.), The Crato Fossil Beds of Brazil: Window into an Ancient World. Cambridge: Cambridge University Press, 133-141. https://doi.org/10.1017/CBO9780511535512.011

Scotese, C.R., 2014. Atlas of Early Cretaceous Paleogeographic Maps, PALEOMAP Atlas for ArcGIS, volume 2, The Cretaceous, Maps 23 - 31, Mollweide Projection, PALEOMAP Project, Evanston, IL. PALEOMAP Project, Evanston, IL. https://doi.org/10.13140/2.1.4099.4560

Scotese, C.R., Moore, T.L., 2014. Atlas of Phanerozoic Ocean Currents and Salinity (Mollweide Projection), Volumes 1-6, PALEOMAP Project PaleoAtlas for ArcGIS, PALEOMAP Project, Evanston, IL. https://www.researchgate.net/publication/267511712_Atlas_of_Phanerozoic_Ocean_Currents_and_Salinity_Mollweide_Projection_Volumes_1-6_PALEOMAP_Project_PaleoAtlas_for_ArcGIS_PALEOMAP_Project_Evanston_IL

Selby D., Creaser R.A., 2003. Re-Os geochronology of organic rich sediments: an evaluation of organic matter analysis methods. Chemical Geology 200, 225-240. https://doi.org/10.1016/S0009-2541(03)00199-2

Selby D., Creaser R.A., 2005a. Direct radiometric dating of hydrocarbon deposits using rhenium-osmium isotopes. Science 308, 1293-1295. https://doi.org/10.1126/science.1111081

Selby D., Creaser R.A., 2005b. Direct radiometric dating of the Devonian-Mississippian time-scala boundary using the Re-Os black shale geochronometer. Geology 33, 545-548. https://doi.org/10.1130/G21324.1

Selby, D., 2007. Direct Rhenium-Osmium age of the Oxfordian-Kimmeridgian boundary, Staffin bay, Isle of Skye, U.K., and the late Jurassic time scale. Norwegian Journal of Geology 87(3), 291-299. https://www.researchgate.net/publication/285745042_Direct_Rhenium-Osmium_age_of_the_Oxfordian-Kimmeridgian_boundary_Staffin_bay_Isle_of_Skye_UK_and_the_Late_Jurassic_time_scale

Selby, D., Creaser, R.A., Stein, H.L., Markey, R.J., Hannah, J.L., 2007. Assessment of the ^{187}Re decay constant by cross calibration of Re-Os molybdenite and U-Pb zircon chronometers in magmatic ore systems. Geochimica et Cosmochimica Acta 71, 1999-2013. https://doi.org/10.1016/j.gca.2007.01.008

Selby, D., Mutterlose, J., Condon, D.J., 2009. U-Pb And Re-Os Geochronology of the Aptian/Albian and Cenomanian/Turonian stage boundaries: Implications for timescale calibration, osmium isotope seawater composition and Re-Os systematics in organic-rich sediments. Chemical Geology 265, 394-409. https://doi.org/10.1016/j.chemgeo.2009.05.005

Sharma, M., Wasserburg, G.J., Hofmann, A.W., Chakrapani, G.J., 1999. Himalayan uplift and osmium isotopes in oceans and rivers. Geochimica et Cosmochimica Acta 63, 4005-4012. https://doi.org/10.1016/S0016-7037(99)00305-1

Silva, M.A.M., 1986. Lower Cretaceous unconformity truncating evaporite-carbonate sequence, Araripe Basin, Northeastern Brazil. Revista Brasileira de Geociências 16(3), 306-310. http://www.ppegeo.igc.usp.br/index.php/rbg/article/view/12012

Silva, M.D., 1975. Primeira ocorrência de charophyta na Formação Santana (Cretáceo) do Grupo Araripe, nordeste do Brasil. VII Simpósio de Geologia do NE, Fortaleza, Brasil, 67-73.

Silva, L.C., McNaughton, N.J., Vasconcelos, A.M., Gomes, J.R.C., Fletcher, I.R., 1997. U-Pb SHRIMP ages in southern State of Ceará, Borborema province, NE Brazil: Archean TTG accretion and Proterozoic crustal reworking. 2 th International Symposium on Granites and Associated Mineralizations, 280-281.

Silva, T.L.S., Mendes, P.R.C., Castro, R.G., Pereira, R., Souza Neto, J.A., Fambrini, G.L., 2014. Caracterização geoquímica de folhelhos betuminosos da Formação Ipubi, Bacia do Araripe por meio de *n*-alcanos e isoprenoides. 47º Congresso Brasileiro de Geologia, Salvador, Brasil. https://www.researchgate.net/publication/334151694_CARACTERIZACAO_GEOQUIMICA_DOS_FOLHELHOS_PIROBETUMINOSOS_DA_FORMACAO_IPUBI_BACIA_DO_ARARIPE_POR_MEIO_DE_n-ALCANOS_E_ISOPRENOIDES

Silva-Telles Jr., A.C., Vianna, M.S.S., 1990. Paleoecologia dos ostracodes da Formação Santana (Bacia do Araripe): Um estudo ontogenético de populações. I Simpósio Bacia Araripe e Bacias Interiores Nordeste, Crato, Brasil.

Smoliar, M.I., Walker, R.J., Morgan, J.W., 1996. Re-Os Ages of Group IIA, IIIA, IVA, and IVB Iron Meteorites. Science 271, 1099-1102. https://www.jstor.org/stable/2889840

Souza Neto, J.A., Vortisch, W.B., Mort, H.P., Valença, L.M.M., Barbosa, J.A., Neumann, V.H.M.L., Miranda, T.S., Correia Filho, O.J., Brandao, P.A.L.S., Moriel, I.S., 2013. Mineralogical and chemical characterization of clay minerals filling gypsum-rich veins crosscutting the evaporite sequence of the Ipubi Formation, Araripe Basin, northeastern Brazil. XV International Clay Conference, Rio de Janeiro, Brasil. https://tiagomirandaorg.files.wordpress.com/2016/12/799_souza_neto_et_al_xv_icc_2013_fractures.pdf

Sucerquia, P.A., Bernardes-de-Oliveira, M.E.C., Mohr, B.A.R., 2015. Phytogeographic, stratigraphic and paleoclimatic significance of *Pseudofrenelopsis capillata* sp. nov. from the Lower Cretaceous Crato Formation, Brazil. Review of Palaeobotany and Palynology 222, 116-128. https://doi.org/10.1016/j.revpalbo.2015.07.012

Tejada, M.L.G., Suzuki, K., Kuroda, J., Coccioni, R., Mahoney, J.J., Ohkouchi, N., Sakamoto, T., Tatsumi, Y., 2009. Ontong Java Plateau eruption as a trigger for the Early Aptian oceanic anoxic event. Geology 37, 855-858. https://doi.org/10.1130/G25763A.1

Tomé, M.E.R.T., Lima Filho, M.F., Neumann, V.H.M.L., 2014. Taxonomic studies of non-marine ostracods in the Lower Cretaceous (Aptian-Lower Albian) of post-rift sequence from Jatobá and Araripe basins (Northeast Brazil): Stratigraphic implications. Cretaceous Research 48, 153-176. https://doi.org/10.1016/j.cretres.2013.12.007

Tribovillard, N., Algeo, T.J., Lyons, T., Riboulleau, A., 2006. Trace metals as paleoredox and paleoproductivity proxies: An update. Chemical Geology 232, 12-32. https://doi.org/10.1016/j.chemgeo.2006.02.012

Tripathy, G.R., Hannah, J.L., Stein, H.J., Yang, G., 2014. Re–Os age and depositional environment for black shales from the Cambrian–Ordovician boundary, Green Point, western Newfoundland. Geochem. Geophys. Geosyst.15, 1021–1037. http://dx.doi.org/10.1002/2013GC005217.

Tripathy, G.R., Hannah, J.L., Stein, H.J., Geboy, N.J., Ruppert, L.F., 2015. Radiometric dating of marine-influenced coal using Re–Os geochronology. Earth and Planetary Science Letters 432, 13-23. http://dx.doi.org/10.1016/j.epsl.2015.09.030

Tripathy, G.R., Singh, S.K., 2015. Re-Os depositional age for black shales from the Kaimur Group, Upper Vindhyan, India. Chemical Geology 413, 63-72. https://doi.org/10.1016/j.chemgeo.2015.08.011

Unwin, D., Martill, D., 2007. Pterosaurs of the Crato Formation. In: Martill, D.M., Bechly, G., Loveridge, R. (Eds.), The Crato Fossil Beds of Brazil: Window into an Ancient World. Cambridge: Cambridge University Press, 475-524. https://doi.org/10.1017/CBO9780511535512.018

Vallati, P., 2013. A Mid-Cretaceous palynoflora with *tucanopollis crisopolensis* from D-129 Formation, San Jorge Gulf Basin, Argentina. Revista Brasileira de Paleontologia 16(2), 237-244. https://10.4072/rbp.2013.2.06

Vale, J.A.R., 2018. Caracterização geoquímica e geocronológica do Complexo Granjeito, Província da Borborema, NE Brasil: implicações para a evolução crustal paleoarqueana do distrito ferrífero de Curral Novo do Piauí (PhD thesis). Universidade de São Paulo, 131 pp. https://doi.org/10.11606/D.44.2019.tde-30052019-103844

Warren, J.K. (Ed.), 2016. Evaporites a Geological Compendium. Springer, Switzerland, 1813 pp. https://doi.org/10.1007/978-3-319-13512-0

Witton, M.P., 2007. Titans of the skies: Azhdarchid pterosaurs. Geology Today 23, 33-38. https://doi.org/10.1111/j.1365-2451.2007.00596.x

Woodhouse, O., Ravizza, G., Falkner, K.K., Statham, P., Peucker-Ehrenbrink, B., 1999, Osmium in seawater: vertical profiles of concentration and isotopic composition in the eastern Pacifc Ocean. Earth and Planetary Science Letters.173, 223-233. https://doi.org/10.1016/S0012-821X(99)00233-2

Xu, W., Ruhl, M., Jenkyns, H.C., Hesselbo, S.P., Riding, J.B., Selby, D., Naafs, B.D.A., Weijers, J.W.H., Pancost, R.D., Tegelaar, E.W., Idiz, E.F., 2017. Carbon sequestration in an expanded lake system during the Toarcian oceanic anoxic event. Nature Geoscience 10, 129-134. https://www.nature.com/articles/ngeo2871

Yang, G., Hannah, J., Zimmerman, A., Stein, H., Bekker, A., 2009. Re–Os depositional age for Archean carbonaceous slates from the southwestern Superior Province: challenges and insights. Earth and Planetary Science Letters 280, 83–92.

York, D., 1969. Least-squares fitting of a straight line with correlated errors. Earth and Planetary Science Letters 5, 320-324. https://doi.org/10.1016/S0012-821X(68)80059-7

FIGURE CAPTIONS

Fig. 1. Location of the Araripe Basin (highlighted by the red box) within the geotectonic context of the Borborema Province. MCD: Médio Coreaú Domain; CD: Cearence Domain; RGND: Rio Grande do Norte Domain; TZD: Transversal Zone Domain; SD: South Domain (Modified from Matos, 1999; Medeiros, 2004).

Fig. 2. Simplified map of the Araripe Basin to represent sampling location (Modified from Assine, 2007).

Fig. 3. Schematic stratigraphic profile and micropaleontology assemblage of the Santana Group, Araripe Basin (based in Coimbra et al., 2002; Tomé et al., 2014).

Fig. 4. Sampling strategy and composite stratigraphy of the 1m interval sampled of the Ipubi Formation black shale. (A and B) The Ipubi Formation black shales were exposed via nine 1 m deep trenches ~4 m apart in the open pit of the Campevi mine. (C) Composite stratigraphic section of the black shale interval exposed (see text for details). (D) Example of fibrous gypsum-filled lens in the upper interval of the black shale profile; (E) fossils within the upper interval of the stratigraphic profile; (F) 30 cm interval of black shale interbedded with marl, and (G) mudstone within the basal 20 cm of the sampled interval.

Fig. 5. Cross-plot of Re (ppb), ^{192}Os (ppt), and enrichment factor of Re and ^{192}Os versus organic matter for the studied samples. See text for discussion.

Fig. 6. Re-Os geochronological results for the Ipubi Formation black shales from the Campevi mine, Brazil. Regression of the Re-Os isotope data together with the 2σ uncertainties in the isotope ratios and the associated error correlation functions (rho) conducted using the beta version of Isochron program (Li et al., 2019), which incorporates the Isoplot algorithm (A, C, E, G) (Ludwig, 2012) and the Monte Carlo method (B, D, F, H). Isoplot data regressions are shown for all data (A), and with only sample TM09 excluded (C), and with samples TM05 and TM09 excluded (E), and with samples TM05, TM06 and TM09 excluded (G). Monte Carlo approach distribution of age and initial ^{187}Os/^{188}Os values are show in B (all data), D (TM09 excluded), F (TM05 and TM09 excluded), and H (TM05, TM06 and TM09 excluded). The inset shows total uncertainty at the 2 sigma level and the contribution to the total uncertainty from the analytical uncertainty. Bracketed age uncertainties include the uncertainty on the decay constant. See text for discussion.

Fig. 7. A new chronostratigraphic proposal for the deposition of the lithostratigraphic units of the Post-Rift I sequence (Santana Group) of the Araripe Basin based on both regional observations (Assine et al., 2014; Neumann and Assine, 2015; Custódio et al., 2017) and the Re-Os age presented in this study.

Fig. 8. Aptian paleogeographic and paleoceanographic map illustrating the western Tethys Sea incursion in the northeast Brazilian basins. The red arrows represent the

paleocirculation during this period. The Araripe Basin is represented by the yellow star, and the São Luís and Parnaíba basins are represented by the purple and orange star, respectively (modified after Scotese, 2014; Scotese and Moore, 2014; Arai, 2014).

Table 1: Synopsis of organic matter, $CaCO_3$ and aluminium content, enrichment factor data, and Re-Os data for the samples from Ipubi Formation black shale.

Batch/Sample	Lithology	$CaCO_3$ (%)	OM (%)	Al (ppm)	Re (EF)#	^{192}Os (EF)#	Re (ppb)	±	Os (ppt)^	±	^{192}Os (ppt)	±	$^{187}Re/^{188}Os$	±	$^{187}Os/^{188}Os$	±	rho	% Re Blank	% ^{187}Os Blank	% ^{188}Os Blank	Os_i @ 130 myr*	Os_i @ 125 myr*	Os_i @ 124 myr*	Os_i @ 123 myr*	±
TM01	Black Shale	24.5	15.5	64565.7	2.5	689.0	2.2	0.006	69.4	0.4	22.2	0.1	197.2	1.2	2.362	0.019	0.654	0.68	0.01	0.15	1.93	1.95	1.96	1.96	0.02
TM02	Mudstone	24.6	12.3	58397.8	1.6	819.9	1.3	0.004	73.3	0.6	23.9	0.2	108.4	1.0	2.181	0.027	0.677	1.00	0.02	0.17	1.95	1.96	1.96	1.96	0.03
TM03	Black Shale interbedded Marl	43.1	17.9	11182.5	219.9	13741.5	33.7	0.082	273.5	1.6	76.6	0.3	875.6	4.0	3.757	0.020	0.606	0.08	0.01	0.10	1.86	1.93	1.95	1.96	0.03
TM04	Black Shale interbedded Marl	42.1	13.0	6245.9	309.8	22864.5	26.5	0.065	248.2	1.4	71.2	0.3	741.2	3.4	3.489	0.019	0.609	0.10	0.01	0.11	1.88	1.94	1.96	1.97	0.02
TM05	Black Shale interbedded Marl	44.2	18.3	8424.5	180.8	16525.3	20.9	0.051	237.2	1.4	69.4	0.3	598.4	2.7	3.276	0.018	0.610	0.12	0.01	0.12	1.98	2.03	2.04	2.05	0.02
TM06	Black Shale interbedded Marl	45.8	15.5	4802.9	378.3	28062.1	24.9	0.062	234.9	1.4	67.2	0.3	737.4	3.4	3.522	0.019	0.609	0.10	0.01	0.12	1.92	1.99	2.00	2.01	0.02
TM07	Mudstone	37.5	5.1	17730.9	3.1	9703.3	0.7	0.003	26.8	0.2	8.6	0.1	174.0	1.8	2.333	0.031	0.704	1.73	0.05	0.47	1.96	1.97	1.97	1.98	0.03
TM08	Mudstone	34.5	6.1	23893.2	3.1	835.0	1.0	0.003	31.3	0.3	10.0	0.1	204.4	2.1	2.405	0.031	0.697	1.27	0.04	0.40	1.96	1.98	1.98	1.99	0.03
TM09	Mudstone	23.8	12.6	64566.5	0.7	440.5	0.6	0.002	42.4	0.3	14.2	0.1	85.5	0.9	1.922	0.024	0.657	2.13	0.04	0.28	1.74	1.74	1.75	1.75	0.03

^Total Os abundance.

#EF is the Enrichment Factor where $EF_{element}$ X = (X ÷ Al sample) ÷ (X ÷ Al upper crust) (Algeo and Maynard, 2004; Tribovillard et al., 2006).

*Os_i = the calcuated initial $^{187}Os/^{188}Os$ composition at a given depositional age.

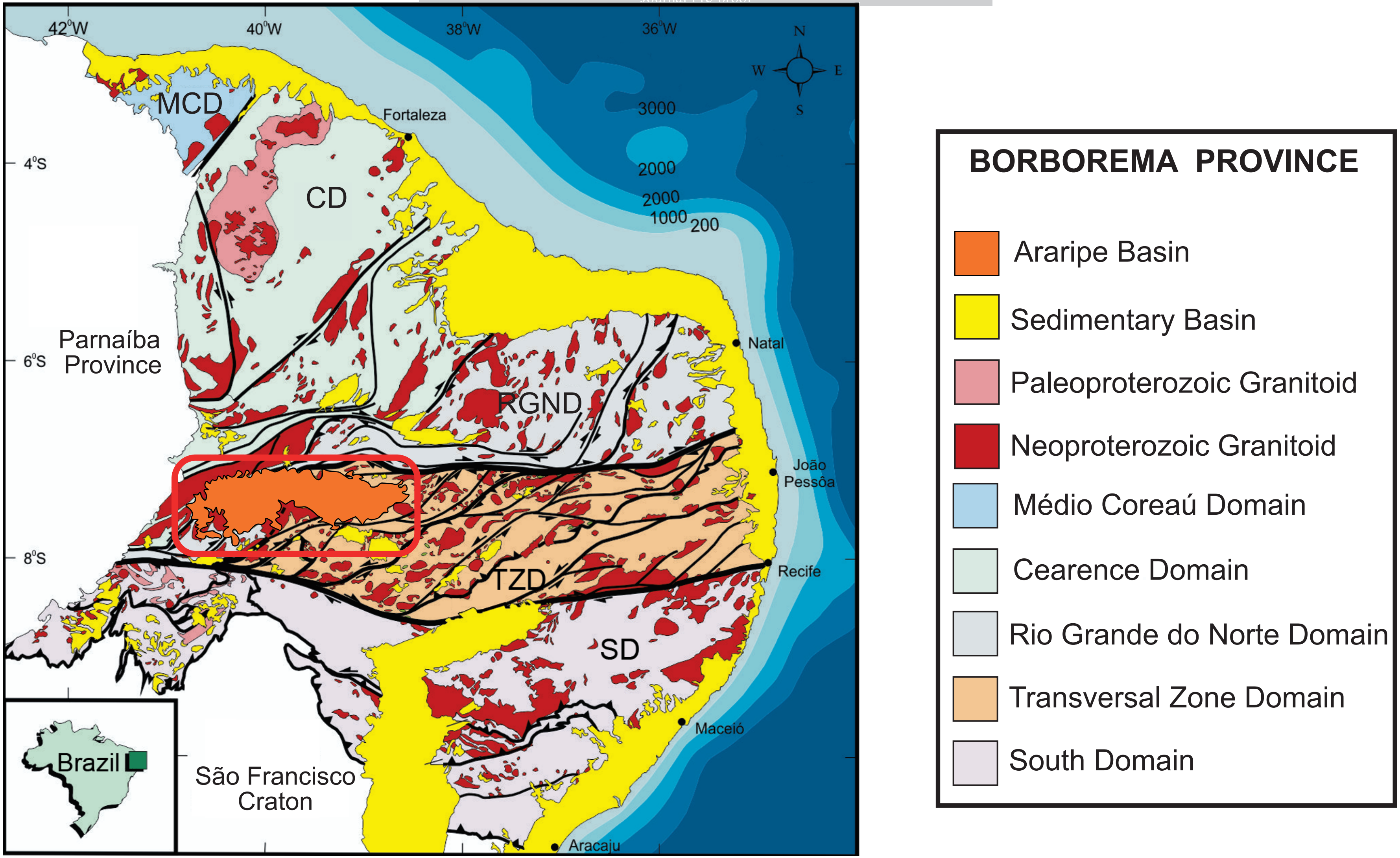
42°W
40°W
38°W
36°W
N
W
E
S
4°S
6°S
8°S
MCD
CD
Fortaleza
3000
2000
2000
1000
200
Parnaíba
Province
RGND
Natal
João
Pessôa
TZD
Recife
SD
Maceió
Brazil
São Francisco
Craton
Aracaju
BORBOREMA PROVINCE
Araripe Basin
Sedimentary Basin
Paleoproterozoic Granitoid
Neoproterozoic Granitoid
Médio Coreaú Domain
Cearence Domain
Rio Grande do Norte Domain
Transversal Zone Domain
South Domain

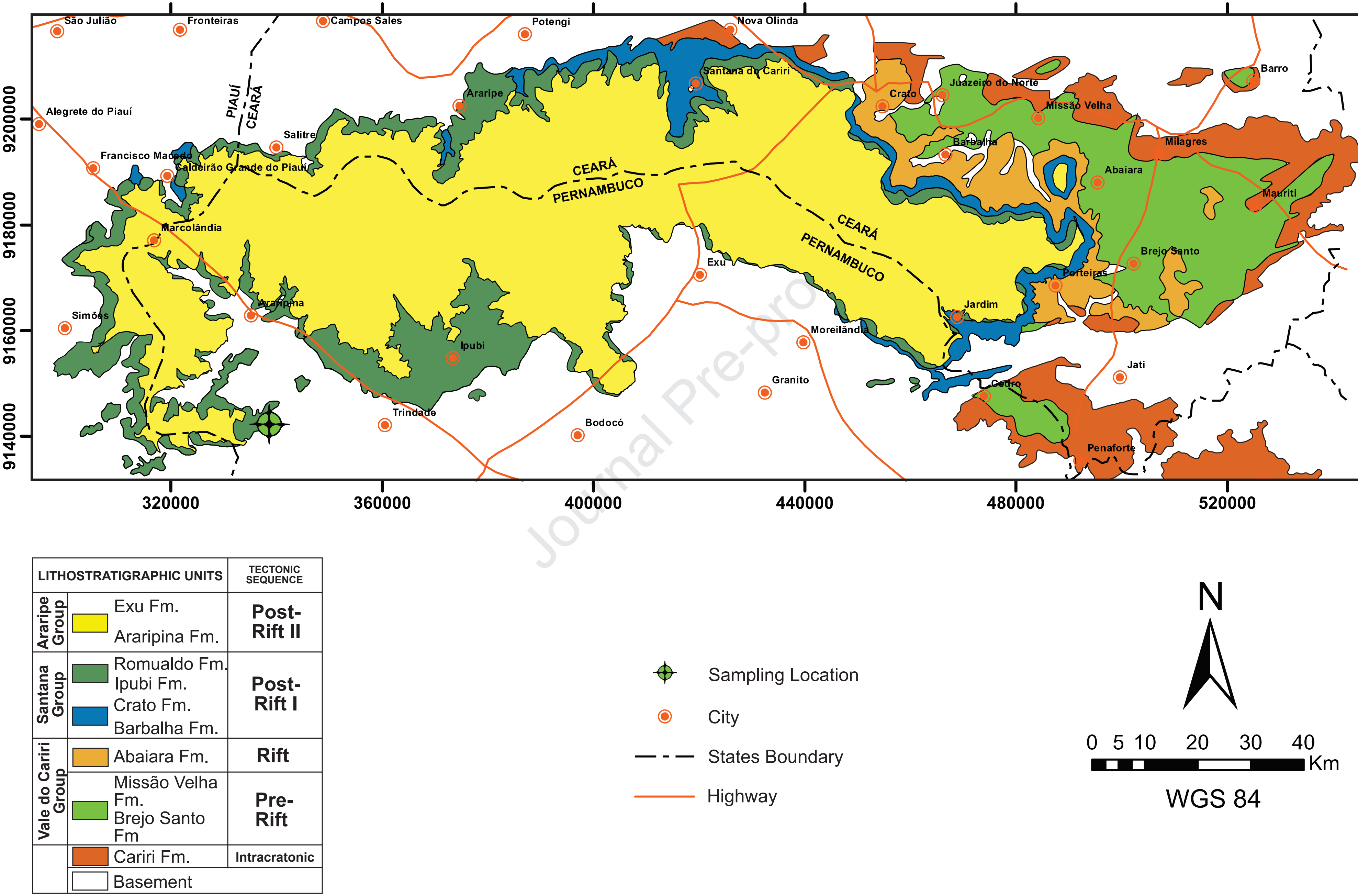

320000
360000
400000
440000
480000
520000
9200000
9180000
9160000
9140000
São Julião
Fronteiras
Campos Sales
Potengi
Nova Olinda
Santana do Cariri
Barro
Juazeiro do Norte
Crato
Araripe
Missão Velha
Alegrete do Piauí
Salitre
Barbalha
Milagres
Francisco Macedo
Caldeirão Grande do Piauí
Abaiara
Mauriti
Marcolândia
Brejo Santo
Exu
Porteiras
Araripina
Jardim
Simões
Ipubi
Moreilândia
Jati
Granito
Cedro
Trindade
Bodocó
Penaforte
PIAUÍ
CEARÁ
PERNAMBUCO
LITHOSTRATIGRAPHIC UNITS
TECTONIC SEQUENCE
Araripe Group
Exu Fm.
Araripina Fm.
Post-Rift II
Santana Group
Romualdo Fm.
Ipubi Fm.
Crato Fm.
Barbalha Fm.
Post-Rift I
Vale do Cariri Group
Abaiara Fm.
Rift
Missão Velha Fm.
Brejo Santo Fm
Pre-Rift
Cariri Fm.
Intracratonic
Basement
Sampling Location
City
States Boundary
Highway
N
0 5 10 20 30 40
Km
WGS 84

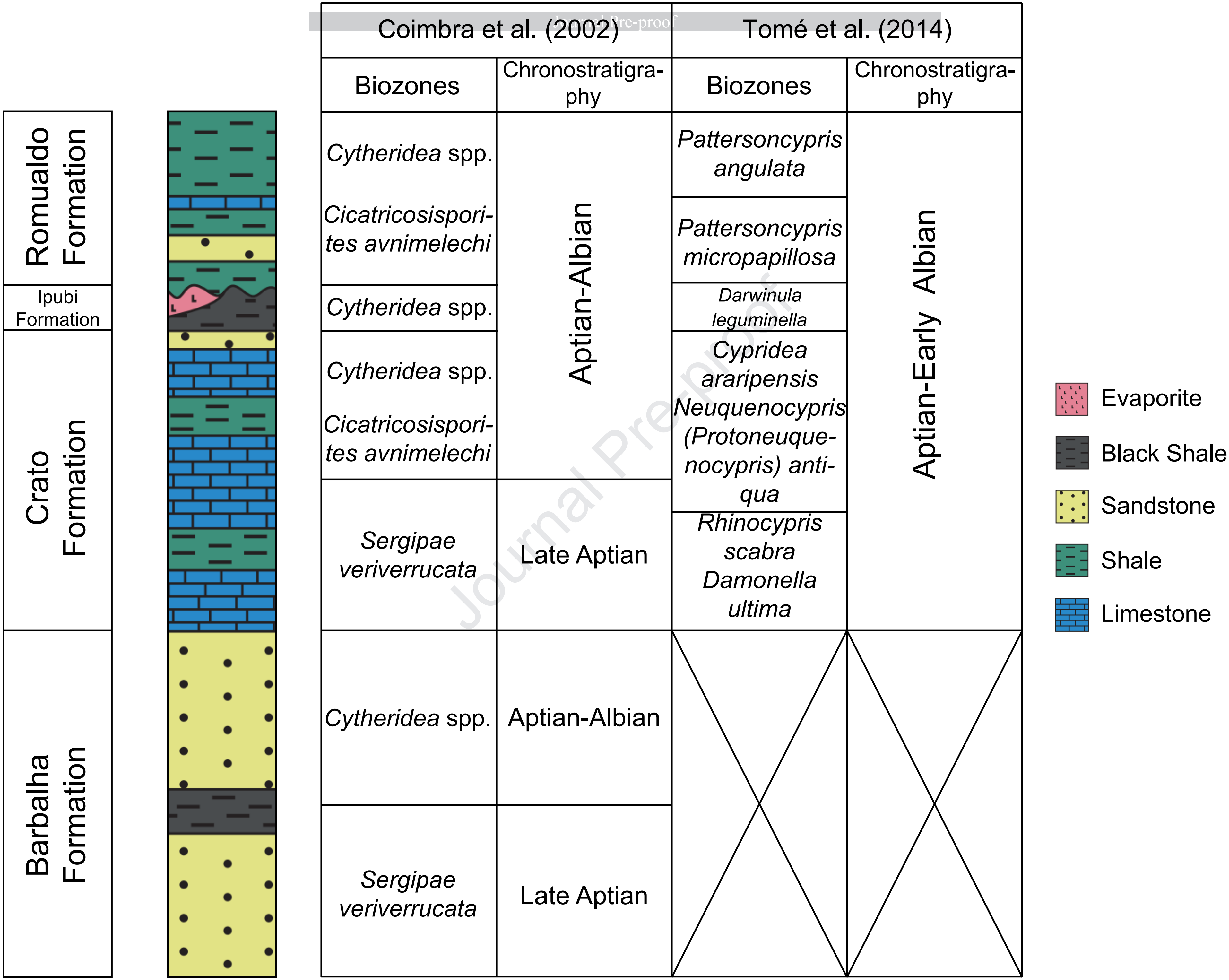
Coimbra et al. (2002)
Tomé et al. (2014)
Biozones
Chronostratigraphy
Biozones
Chronostratigraphy
Romualdo Formation
Ipubi Formation
Crato Formation
Barbalha Formation
Cytheridea spp.
Cicatricosisporites avnimelechi
Cytheridea spp.
Cytheridea spp.
Cicatricosisporites avnimelechi
Aptian-Albian
Sergipae veriverrucata
Late Aptian
Cytheridea spp.
Aptian-Albian
Sergipae veriverrucata
Late Aptian
Pattersoncypris angulata
Pattersoncypris micropapillosa
Darwinula leguminella
Cypridea araripensis
Neuquenocypris (Protoneuquenocypris) antiqua
Rhinocypris scabra
Damonella ultima
Aptian-Early Albian
Evaporite
Black Shale
Sandstone
Shale
Limestone

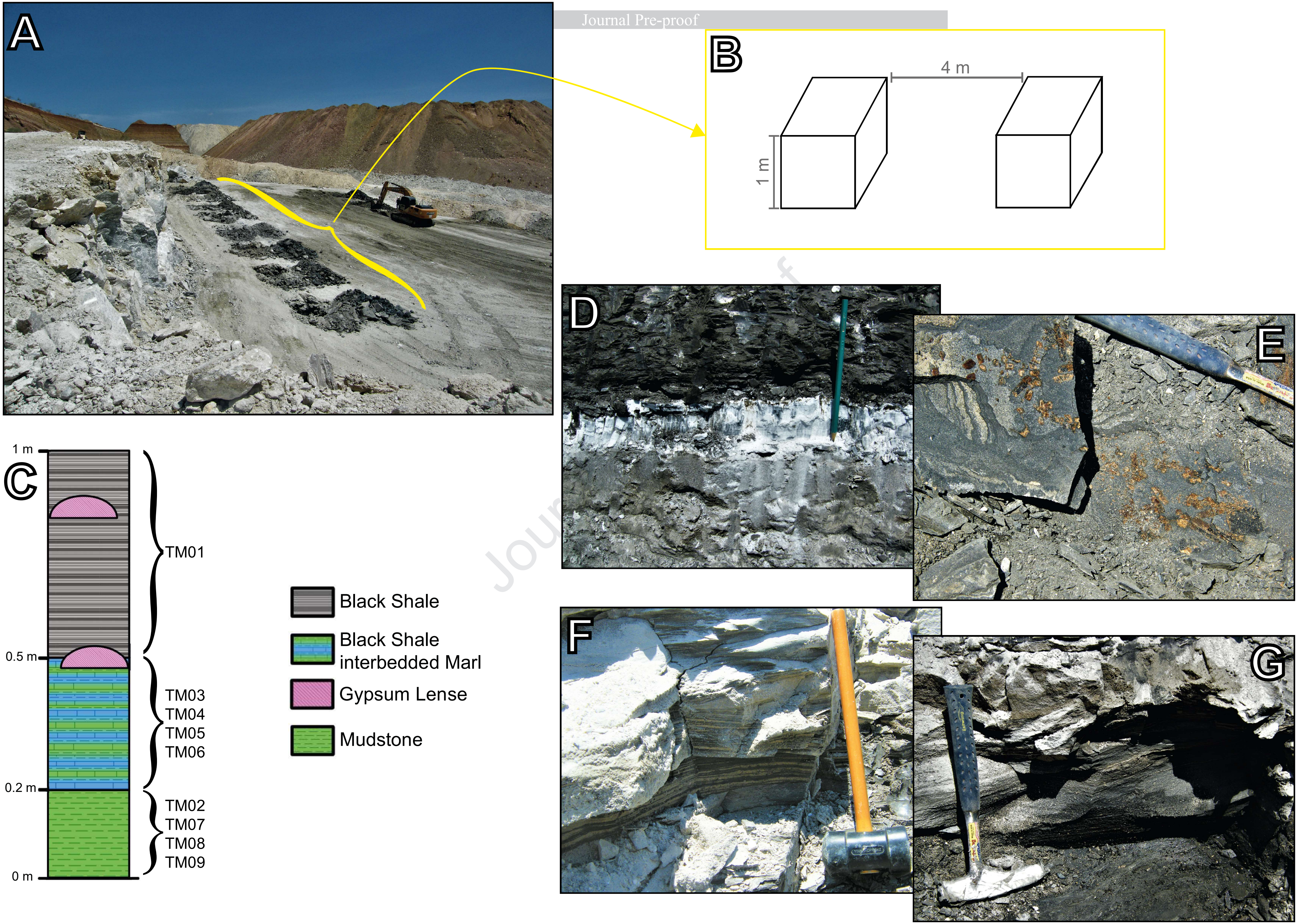
A
B
4 m
1 m
C
1 m
0.5 m
0.2 m
0 m
TM01
TM03
TM04
TM05
TM06
TM02
TM07
TM08
TM09
Black Shale
Black Shale interbedded Marl
Gypsum Lense
Mudstone
D
E
F
G

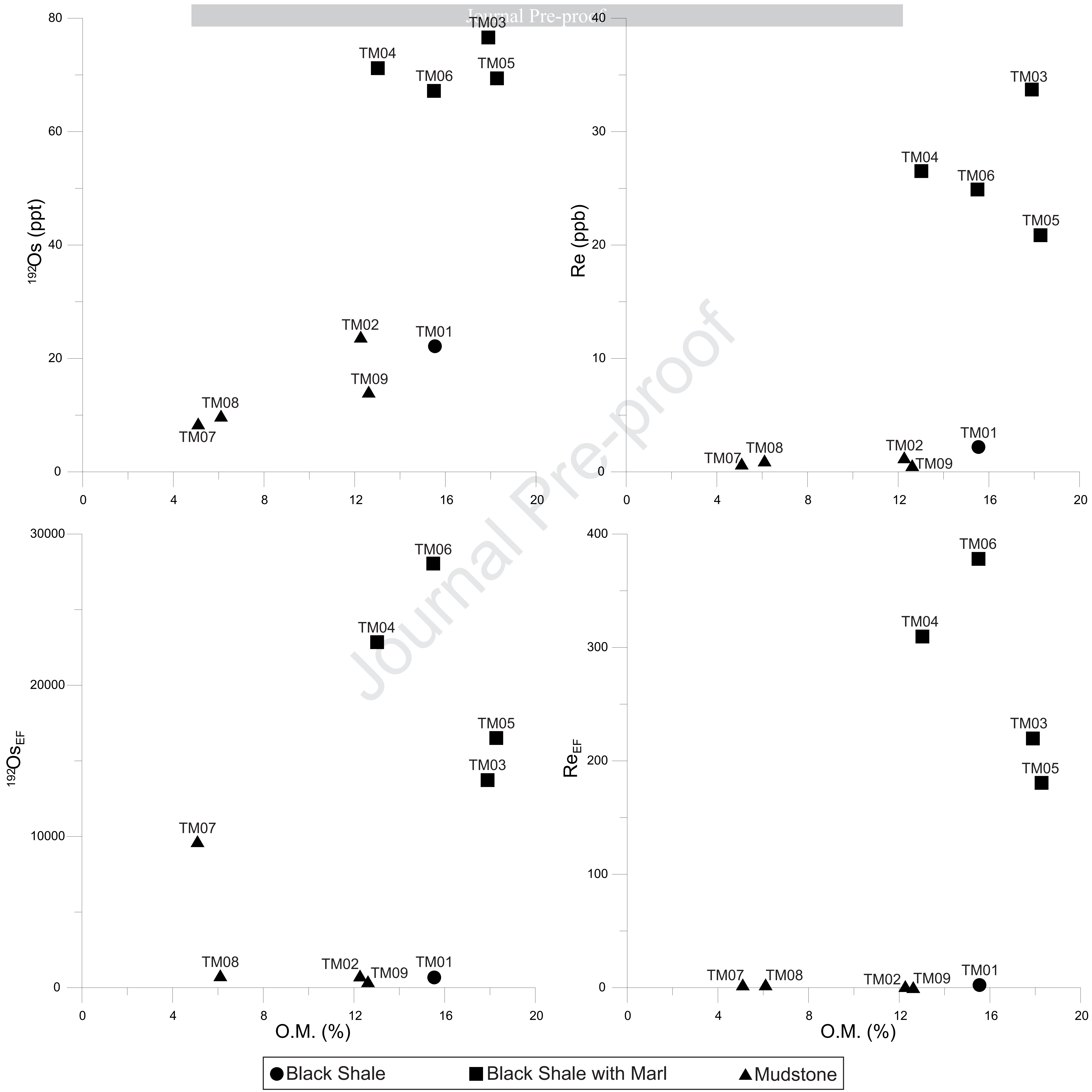

192Os (ppt)
Re (ppb)
192OsEF
ReEF
O.M. (%)
TM01
TM02
TM03
TM04
TM05
TM06
TM07
TM08
TM09
Black Shale
Black Shale with Marl
Mudstone

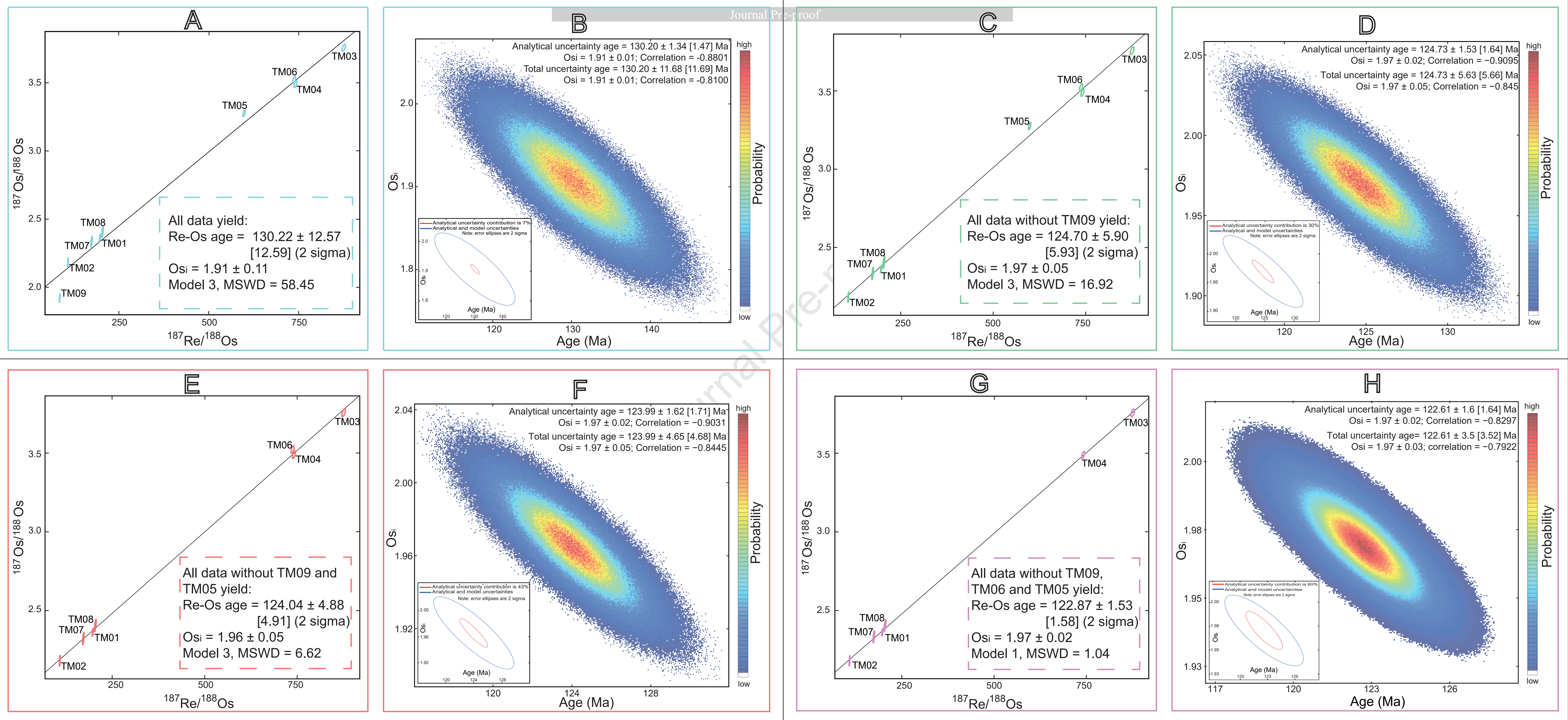
A
187Os/188Os
187Re/188Os
TM03
TM06
TM04
TM05
TM08
TM07
TM01
TM02
TM09
All data yield:
Re-Os age = 130.22 ± 12.57
[12.59] (2 sigma)
Osi = 1.91 ± 0.11
Model 3, MSWD = 58.45
B
Analytical uncertainty age = 130.20 ± 1.34 [1.47] Ma
Osi = 1.91 ± 0.01; Correlation = -0.8801
Total uncertainty age = 130.20 ± 11.68 [11.69] Ma
Osi = 1.91 ± 0.01; Correlation = -0.8100
Osi
Age (Ma)
Probability
high
low
C
187Os/188Os
187Re/188Os
TM03
TM06
TM04
TM05
TM08
TM07
TM01
TM02
All data without TM09 yield:
Re-Os age = 124.70 ± 5.90
[5.93] (2 sigma)
Osi = 1.97 ± 0.05
Model 3, MSWD = 16.92
D
Analytical uncertainty age = 124.73 ± 1.53 [1.64] Ma
Osi = 1.97 ± 0.02; Correlation = −0.9095
Total uncertainty age = 124.73 ± 5.63 [5.66] Ma
Osi = 1.97 ± 0.05; Correlation = −0.845
Osi
Age (Ma)
Probability
high
low
E
187Os/188Os
187Re/188Os
TM03
TM06
TM04
TM08
TM07
TM01
TM02
All data without TM09 and
TM05 yield:
Re-Os age = 124.04 ± 4.88
[4.91] (2 sigma)
Osi = 1.96 ± 0.05
Model 3, MSWD = 6.62
F
Analytical uncertainty age = 123.99 ± 1.62 [1.71] Ma
Osi = 1.97 ± 0.02; Correlation = −0.9031
Total uncertainty age = 123.99 ± 4.65 [4.68] Ma
Osi = 1.97 ± 0.05; Correlation = −0.8445
Osi
Age (Ma)
Probability
high
low
G
187Os/188Os
187Re/188Os
TM03
TM04
TM08
TM07
TM01
TM02
All data without TM09,
TM06 and TM05 yield:
Re-Os age = 122.87 ± 1.53
[1.58] (2 sigma)
Osi = 1.97 ± 0.02
Model 1, MSWD = 1.04
H
Analytical uncertainty age = 122.61 ± 1.6 [1.64] Ma
Osi = 1.97 ± 0.02; Correlation = −0.8297
Total uncertainty age= 122.61 ± 3.5 [3.52] Ma
Osi = 1.97 ± 0.03; correlation = −0.7922
Osi
Age (Ma)
Probability
high
low


30° N
North America
Western
Tethys Sea
Tethys
Sea
0°
Africa
South America
30° S
India

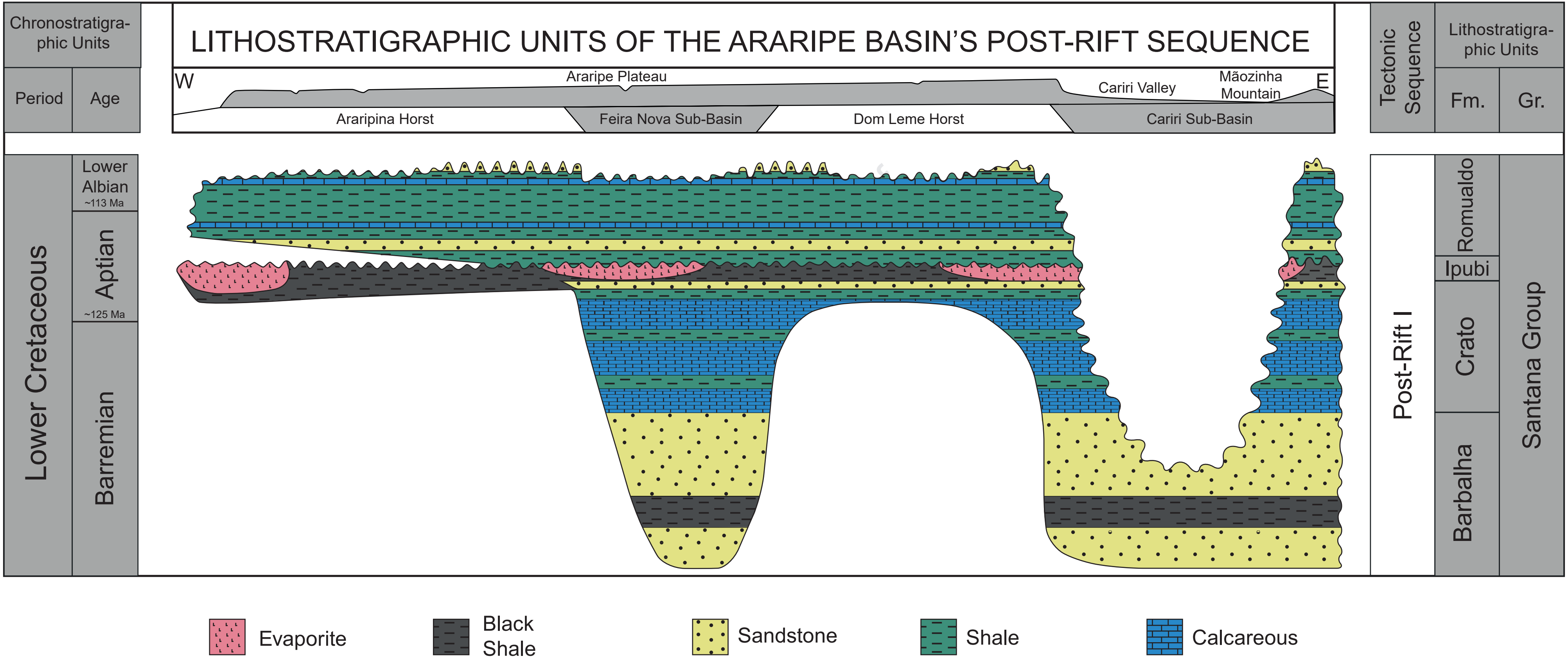
LITHOSTRATIGRAPHIC UNITS OF THE ARARIPE BASIN'S POST-RIFT SEQUENCE
Chronostratigraphic Units
Period
Age
W
Araripe Plateau
Cariri Valley
Mãozinha Mountain
E
Araripina Horst
Feira Nova Sub-Basin
Dom Leme Horst
Cariri Sub-Basin
Tectonic Sequence
Lithostratigraphic Units
Fm.
Gr.
Lower Cretaceous
Lower Albian
~113 Ma
Aptian
~125 Ma
Barremian
Post-Rift I
Romualdo
Ipubi
Crato
Barbalha
Santana Group
Evaporite
Black Shale
Sandstone
Shale
Calcareous

The Highlights considered for the manuscript are:

1. The first Re-Os absolute age (123 ± 3.5 Ma) for Ipubi Formation black shales in the Araripe Basin indicates the formation is Late Barremian / Early Aptian and not Aptian / Albian, and was deposited prior to the onset of OAE1a.

2. Based on the Re-Os age a new chronostratigraphic model is proposed for the Santana Group, Araripe Basin.

3. Highly radiogenic $^{187}Os/^{188}Os$ compositions of 1.97 ± 0.02 imply that the Araripe Basin records a highly restricted water mass during the Late Barremian / Early Aptian.

AUTHORS CONTRIBUTIONS

THALES LÚCIO: Conceptualization; Validation; Formal analysis; Resources; Writing - Original Draft; Writing - Review & Editing; Visualization.

JOÃO ADAUTO SOUZA NETO: Conceptualization; Validation; Writing - Review & Editing; Project administration; Funding acquisition.

DAVID SELBY: Conceptualization; Methodology; Validation; Formal analysis; Investigation; Resources; Data Curation; Writing - Original Draft; Writing - Review & Editing; Supervision; Project administration.

Conflict of Interest

February 18, 2020

Editorial Department of Journal of South American Earth Sciences

Dear Editor-in-Chief,

We strongly request that the manuscript is not reviewed by any member of the AIRIE research group led by Holly Stein at Colorado State University because of the previous publication history and importantly at present Holly Stein and co-workers are working in the same competitive area, and there is a potential for conflict of interest.

Thank you for your consideration and we look forward to hearing from you.

Sincerely,

Thales Lúcio, PhD Student

Geochemistry Laboratory Applied to Petroleum
Department of Geology
Graduate Program in Geosciences, Federal University of Pernambuco
Avenida da Arquitetura, s/n, Cidade Universitária
Recife, Pernambuco, CEP: 50.740-550, Brazil
Tel.: +55-81-21268240; Fax: +55-81-21268234; e-mail: thaales.lucio@gmail.com